UNIVERSITA' DEGLI STUDI DI PADOVA

DOCTORAL THESIS
DOCTORAL SCHOOL OF CROP SCIENCES
CURRICULUM OF ENVIRONMENTAL AGRONOMY, CYCLE XXII
Department of Environmental Agronomy and Crop Production

MONITORING DESERTIFICATION IN SUDAN USING REMOTE SENSING AND GIS

Head of the School: Prof. Dr. Andrea Battisti _____

Supervisor: Prof. Dr. Francesco Morari _____

Doctoral Student: Mona Abdelhafeez Ahmed Dawelbait

_____

THESIS SUBMISSION DATE
1st February 2010

Declaration

I hereby declare that this submission is my own work and that, to the best of my knowledge and belief, it contains no material previously published or written by another person nor material which to a substantial extent has been accepted for the award of any other degree or diploma of the university or other institute of higher learning, except where due acknowledgment has been made in the text.

_____/Mona Abdelhafeez Ahmed Dawelbait /_____

A copy of the thesis will be available at *http://paduaresearch.cab.unipd.it/*

Dichiarazione

Con la presente affermo che questa tesi è frutto del mio lavoro e che, per quanto io ne sia a conoscenza, non contiene materiale precedentemente pubblicato o scritto da un'altra persona né materiale che è stato utilizzato per l'ottenimento di qualunque altro titolo o diploma dell'università o altro istituto di apprendimento, a eccezione del caso in cui ciò venga riconosciuto nel testo.

_____/ Mona Abdelhafeez Ahmed Dawelbait /_____

Una copia della tesi sarà disponibile presso *http://paduaresearch.cab.unipd.it/*

Table of Contents

List of Tables

List of Figures

Summary

Remote sensing technology has long been suggested as a time and cost efficient method for observing dryland ecosystem environments, monitoring land cover degradation and characterizing the dynamism of sand dunes. The meaning and value of remote sensing data were enhanced through skilled interpretation, in conjunction with conventionally mapped information and ground-collected data. Spectral Mixture Analysis (SMA) has proved to be a powerful technique to monitor land cover degradation in arid and semi-arid areas. Three Landsat images, acquired in 1987, 1999 and 2008, were analyzed to evaluate desertification processes in three different ecological zones in Sudan (North Kordofan, River Nile and Northern state). Spectral Mixture Analysis (SMA) was adopted using endmembers spectra derived from the image. Multitemporal comparison techniques (visual interpretation and change vector analysis) were applied to estimate the long-term desertification/re-growing and to emphasize land cover variation over time and in space.

Site-specific interactions between natural processes, climate variation and human activity played a pivotal role in desertification; however their interaction was varied according to the ecological zone. In North Kordofan (savannah), desertification significantly prevailed over vegetation re-growth, particularly in areas around rural villages over the last 21 years. Changes in land use and mismanagement of natural resources, mainly caused by deforestation to supply wood for domestic use and overgrazing, were the main driving factors affecting degradation. More than 120,000 km^2 were estimated as being subjected to a medium-high desertification rate. Conversely, the reforestation measures, adopted by the Sudanese Government in the last decade and sustained by higher rainfall, resulted in low-medium re-growth conditions over an area of about 20,000 km^2.

In River Nile (valleys in semi-desert), extreme condition of desertification affected the valleys in the site. Desertification affected an area of 24,482 km^2 as extreme condition and re-growth condition in low status was 1,193 km^2 while most of persistence condition (71,298 km^2) was desert area. Drought and climate variation with the assistance of mismanagement of natural resources were the factors caused desertification, however, human activities were played minor role. In this site the soil is highly vulnerable to wind and water erosion and it was highly increased in 2008.

Irrigated agricultural projects were clearly recognized in Northern State (Valley in desert), with an areas of 28,761 km^2 in low condition. The area affected by desertification was 98,275 km^2 (7,962 km^2 high, 56,075 km^2 medium and 34,239 km^2 low) with 76.40% percentage of the total area. The agricultural projects were at high risk since they were surrounded by desertified areas.

Site-specific strategies which take into account the interactions of the driving factors at local scale are thus necessary to combat desertification, avoiding any implementation of untargeted measures. In order to identify the soundest strategies, high-resolution tools must be applied. In this study the application of SMA to Landsat data appeared to be a consistent, accurate and low-cost technique to obtain information on vegetation cover, soil surface type, and identify risk areas.

Riassunto

La tecnologia di *remote sensing* è stata a lungo considerata un'efficace strumento per l'osservazione di ecosistemi aridi e semi-aridi, il monitoraggio di superfici vegetate degradate e la caratterizzazione delle dinamiche di dune sabbiose. I risultati ottenuti con il *remote sensing* sono stati validati grazie a interpretazioni puntuali, congiuntamente a informazioni mappali classiche e dati raccolti in campo. Si è provato, inoltre, che la tecnica denominata Spectral Mixture Analysis (SMA) è un potente strumento per monitorare la degradazione di coperture vegetali in zone aride e semi-aride. In questo studio sono state analizzate tre immagini del satellite Landsat, acquisite nel 1987, 1999 e 2008, al fine di valutare i processi di desertificazione di tre differenti ecosistemi in Sudan (Nord Kordofan, Fiume Nilo e Stato del Nord). La Spectral Mixture Analysis (SMA) è stata impiegata utilizzando *endmembers* ottenuti dall'immagine satellitare e definiti come i diversi componenti di un territorio specifico. Sono state applicate tecniche di comparazione multi temporale (interpretazione visiva dei componenti delle immagini e change vector analysis) per sottolineare la variazione della copertura vegetale e per stimare l'effetto di desertificazione di lungo periodo (o crescita vegetativa) nel tempo e nello spazio.

Le interazioni sito-specifiche tra processi naturali, la variazione delle condizioni climatiche e le attività umane hanno giocato un ruolo centrale nel processo di desertificazione, sebbene le loro interazioni siano diverse nei tre siti studiati. Nel Nord Kordofan (zona di savana) il fenomeno della desertificazione è prevalso in modo significativo sulla crescita vegetativa e in particolar modo nelle aree attorno ai villaggi, nell'ultimo ventennio. Un utilizzo differente dei terreni, così come la mancata gestione delle risorse naturali, causata principalmente dalla deforestazione per la fornitura di legname per uso domestico e l'utilizzo eccessivo delle terre destinate a pascolo, sono stati i principali fattori che hanno determinato la degradazione dell'area. Si è inoltre stimato che più di 120,000 km^2 sono soggetti a un tasso di desertificazione medio - alto. Viceversa, le politiche di riforestazione adottate dal governo sudanese nell'ultimo decennio hanno avuto un impatto medio - basso sul tasso di ricrescita della vegetazione, e in un'area di circa 20,000 km^2.

Nell'area nei pressi del fiume Nilo le vallate oggetto di studio, situate in zone semi-desertiche, sono state estremamente colpite dalla desertificazione. Un intenso fenomeno di desertificazione

ha riguardato un'area di 24,482 km^2, al contrario le condizioni di crescita vegetativa hanno interessato un'area 1,193 km^2. Gran parte del territorio è comunque caratterizzato da condizioni desertiche stabili (71,298 km^2). In questo caso i cambiamenti climatici e la forte siccità, assieme alla mal gestione delle risorse naturali, hanno contribuito alla desertificazione, sebbene l'attività umana sembra aver giocato un ruolo marginale nella degradazione dell'area. In questo sito la degradazione del suolo, altamente vulnerabile all'erosione del vento e dell'acqua, è stata molto alta nell'anno 2008.

Le aree agricole irrigate, invece, erano chiaramente riconoscibili nello Stato del Nord (vallata presente in un sito desertico) e occupavano una superficie di 28,760 km^2. In questo caso l'area è risultata in condizioni scadenti. Il territorio colpito da desertificazione era di 98,275 km^2 (7,962 km^2 tasso alto di desertificazione, 56,075 km^2 tasso medio di desertificazione e 34,239 km^2 tasso basso di desertificazione), corrispondente al 76.40% dell'area totale. Le aree agricole si sono dimostrate ad alto rischio di desertificazione dal momento che erano circondate da zone desertiche.

Da questo quadro si evince che strategie sito-specifiche sono necessarie per combattere la desertificazione, evitando di attuare misure migliorative che non tengano conto degli obiettivi specifici identificati per ogni singola area. Affinché vengano adottate le strategie adeguate è auspicabile l'applicazione di strumenti ad alta risoluzione. Dai risultati di questo studio sembra che l'applicazione della SMA ai dati di Landsat sia coerente, precisa ed economicamente sostenibile al fine di ottenere informazioni utili sulla copertura vegetale, sulle caratteristiche del suolo e sull'identificazione delle aree a rischio.

Dedication

To my mother Alsara, who have taught me the meaning of success
To the soul my father Abdelhafeez who gave me the tools success
To the soul my brother Husain who was keeping pushing me for being succeed

I dedicate this work with a great love and respect

Mona Abdelhafeez A. Dawelbait

PART ONE:
DESERTIFICATION PROCESSES IN ARID AND SEMI-ARID AREAS

1.1 Definitions

Desertification is defined as land degradation in arid, semi-arid and dry sub-humid areas due to climate variation and/or human activity (UNCCD, 1994). The concept of desertification dates back to colonial West Africa in the 1920s and 1930s, and was revived in the early 1970s in an attempt to understand the effects of a long series of drought years that brought environmental degradation, economic difficulty and hunger to the African Sahel (Lonergan, 2005). The concept and emphasis of desertification as a degrading process requiring international collaboration has changed over time. Initially the focus was on desert margins (UNEP, 1986) though there was clear recognition that land degradation was a widespread problem. An accepted definition of the time was that of Dregne (1977): "Desertification is the impoverishment of terrestrial ecosystems under the impact of man. It is a process of deterioration in these ecosystems that can be measured by reduced productivity of desirable plants, undesirable alterations in the biomass and the diversity of the micro and macro flora and fauna, accelerated soil deterioration, and increased hazards for human occupancy". As national and global databases improved, the anthropic role became more evident and the accelerated nature of the process resulted in the call for combating actions.

Arid and semi-arid areas are characterized by patterns of variable annual rainfall. They include the deserts and their semi-arid and sub-humid dry margins and the subtropical Mediterranean latitudes. Arid zones account for 40% of the Earth’s surface. Because of the vast area covered these lands play a major role in energy balance and hydrologic, carbon and nutrient cycles. The dryland areas are characterized by irregularity and shortage of rainfall, prolonged dry seasons, high temperature and high evaporation. Such variation in climatic factors makes drylands more fragile and prone to land degradation and desertification (Ayoub. 1998).

Land degradation is one of the effects of mismanagement of land and results frequently from a mismatch between land quality and land use (Beinroth et al., 1994). Land degradation is clearly human induced due to the large area and number of people affected by it. The linkage between land degradation and climate change is yet to be established but there is increasing evidence that land degradation is a driver of climate change (Reich et al., 2001).

Mechanisms of desertification processes could be physical, chemical, and biological processes (Lal, 1994). These processes include water erosion, wind erosion and sedimentation, long-term reduction in diversity of natural vegetation and salinization. Combined pressure from human and climatic variations in arid and semi-arid areas resulted in high and serious desertification

status and rate. Loss of vegetation cover seems to be related to poor soils and aridity, which prevail throughout short as well as long periods of drought and thus permit very limited recovery of natural vegetation. Wind and water erosion are the main two process accelerated in the areas vulnerable to desertification processes in the arid and semi arid regions. They are a result of the interplay between environmental factors such as soil, topography, drainage, rainfall, wind speed, and land use patterns. Main causes accelerate desertification processes are drought, population pressure, failure to implement appropriate technologies, poverty, constraints imposed by recent international trading agreements, and local agricultural and land use policies (Virmani et al., 1994).

Desertification as an environmental degradation phenomenon converts land into desert-like conditions unfit for man and animals. The assumption that desert encroachment is a manifestation of major geological climatically changes is still subject to considerable scientific debate. Most scientists seem to agree that weather fluctuation or cyclic drought of one or more years and land misuses are the actual causes of desertification particularly in arid regions such as is the case in Sudan (Mustafa, 2007).

1.2 Desertification problem in Sudan:

Sudan is the largest country in Africa covering an area of over 2.5 million km^2. Rainfall ranges from nil in the North to 1500 mm y^{-1}in the South. Harrison and Jackson (1958) classified the vegetation of Sudan as ecological terms, according to the floristic composition of the vegetation. However, the structural properties of the vegetation in Sudan are highly depend on rainfall and soil types. Sudan has diverse ecological regions, from the desert in the North to high rainfall woodlands savannas in the South (Ayoub, 2004).

Vegetation in semi arid area in Sudan ranges from extremely scarce in the far north to short grass and sparse thorn scrub to open grassland plains dominated by gum Arabic producing acacia in the central part of the country. The more humid part of the country contains a variety of vegetation types from savannah to broken woodland and tropical forests. Woody biomass comprised 71% of the energy supply in 1999 in the Sudan (Abdel Ati, 2002). This is equivalent to about 400 million *Acacia* trees being uprooted annually. Rangelands in the arid and semi-arid zones carry over 70% of Sudan's livestock. This is more than double their carrying capacity (Ayoub. 1998). Range fires, mostly deliberately set by herders and honey collectors,

consumed annually about 35% of the natural range productivity, estimated to be about 300 million tonnes (Atta El Moula, 1985). Livestock in the Sudan concentrates around water sources during the dry periods leading to vegetation denudation and soil pulverization by tramping (de Jong-Boon, 1990).

Drylands cover approximately 60% of the country (1.5 million km^2), thus constituting the largest area of drylands in Africa. Annual rainfall in arid areas is less than 75 mm and the semi-arid areas with annual rainfall from 75mm to 300mm. These areas faced with serious socio-economic problems such as poverty, famine and migration and environmental problems such as drought, desertification (Khiry, 2007).

Continued drought and desertification are the most important problems facing Sudan as well as North Africa which result mainly from destruction of natural resources, agricultural lands and in political and social disturbances (Mustafa, 2007). Sudan's soil conservation committee in 1994 concluded that soil degradation and desertification is mainly attributed to general land misuses rather than to major climatic changes. human activities are the most destructive factors in Sudan which are leading to natural resources degradation and causing desertification result from droughts, coupled mainly with the extended rainfed farming on marginal lands, overgrazing, wood cutting, deforestation, uprooting of shrubs and burning of grasslands and forest shrubs. DECARP, 1976 concluded that a combination of factors involving fragile ecosystems developed under harsh climatic condition and human activities are the actual causes of desertification in Sudan. Nowadays, the problems of desertification and drought in Sudan are a worldwide concern and specific attention was paid to discussing and combating these impacts particularly in the central part of the country which is severely hit by desertification. Migration to urban areas, deterioration of forest cover, reduction of agricultural production, and famine are the socioeconomic problems face Sudan after severe drought conditions of 1984 (Khiry, 2007).

1.3 Remote sensing and GIS for the monitoring and mapping desertification in arid and semi-arid areas:

Many studies and assessments of dryland ecosystems since the United Nations Conference on Desertification (UNCOD) in 1977 have led to a valuable new understanding of the desertification issue. These studies pointed out significant shortcomings in terms of data and

methodologies. Moreover, they call for the improvement of science and technology for environmental monitoring, assessment models, accurate databases and integrated information systems (Lonergan, 2005). In particular, they emphasize the need to assess desertification processes, since the knowledge on the current status of desertification or the magnitude of the potential hazard is incomplete and fragmented for the most parts of the world. Monitoring of the environment in these areas is considered as a very important task in the context of global climatic change and worldwide desertification dynamics (Lonergan, 2005).

Monitoring desertification is the key tool that can provide timely and useful information for decision makers on the risk of drought and environmental change. It could be easier by determining appropriate indicators. Environmental indicators over large areas must be measurable and suitable for regular updating. Few of the proposed indicators are specifically for dryland degradation only, because it is difficult to separate the effect of the climatic factors from the human activities in such areas (Diouf and Lambin, 2001).

One of the most important tools for monitoring desertification is remote sensing. Ideally, remote sensing should play a major role in developing a global operational capability for monitoring land degradation and desertification in drylands. It has long been suggested as a time and cost efficient method for observing dryland ecosystem environments (Hassan and Luscombe, 1990). Remote sensing is defined as the art of science of obtaining information about the object without being in direct physical contact with the object. It is a technology that can be used to measure and monitor important biophysical and biochemical characteristics of objects, as well as human activities on the Earth (Jensen, 2005). Remote sensing imagery should be regarded as data available to assist the planner in the assessment of natural resource and natural hazard information throughout the development of a planning study. The meaning and value of remote sensing data is enhanced through skilled interpretation used in conjunction with conventionally mapped information and ground-collected data (Jensen, 2005). In this capacity it can serve both enhance monitoring efforts as well as to provide valuable information on dryland degradation in specific area.

In order to monitor, map and model desertification processes, Geographical information system GIS is needed. GIS is a computer-based system for capture, storage, retrieval, analysis and display of spatial (locationally defined) data (The National Science Foundation). GIS id a powerful system to apply the techniques for modeling land cover pattern and erosion indices..

1.4 Problem justification:

Earth observation data, particularly Landsat Thematic Mapper (TM) and Multispectral Scanner (MSS) imagery, have been widely used in semiarid environments to monitor the variations in vegetation community characteristics as well as other factors affecting desertification processes. However, traditional methods to extract vegetation and soil information from remote sensing data in semi-arid areas, such as classification techniques and vegetation indices, were found to be inaccurate due to the vegetation community structure and the heterogeneity of the semi-arid environment. Spectral Mixture Analysis (SMA) has been proposed as an appropriate classification technique to be applied in dryland areas. SMA is sub-pixel classification which based on and influenced by the spectral reflection properties of the land cover materials

The poorly developed communications infrastructure in Sudan pose great difficulty for the collection of data for operational use by a ground based method. Consequently, remote sensing images interpretation and GIS become the feasible tools for timely action on the risk of drought and environmental change.

1.5 Questions of the study?

- How can remote sensing and GIS help in monitoring temporal and spatial variations of vegetation and soil in Sudan?
- Can a limited field data collection suffice to accurately model the pattern of land cover and desertification in Sudan?
- Can long-term and large-scale monitoring of land cover and desertification be useful to improve land management policies?

1.6 Objectives:

- To estimate the desertified lands in three different ecological zones in order determine the status of desertification in Sudan.
- To detect and analyze the dynamics of change of land use/land cover in three different ecological zones using Landsat images and SMA in order to assess the desertification process.

PART TWO:
LIMITS AND POTENTIALITIES OF STUDYING DRYLAND VEGETATION USING THE OPTICAL REMOTE SENSING

Dawelbait, M. and Morari, F., 2008. Limits and potentialities of studying dryland vegetation using the optical remote sensing. Italian Journal of Agronomy 3:97- 106.

Abstract

In optical remote sensing studies, the reflectance of the vegetation canopy in arid and semiarid areas is affected by the optical properties of the vegetation elements, their arrangement in the vegetation canopy and the optical properties of the surrounding environment. The study of vegetation and surrounding environment parameters presents significant peculiarities in arid areas. Low vegetation cover leads to a small contribution of vegetation reflectance in the total pixel reflectance relative to the other materials. Most types of dry ecosystem shrubs do not differ enough from one another to allow discernment of vegetation type. Vegetation in arid and semiarid areas adapts its structure and phenology to the harsh environment, which affects the overall brightness and temporal and spatial interspecies spectral variability. Moreover, the surrounding environment in dry ecosystem influences the reflectance of the vegetation by multiple scattering and nonlinear mixing and variable spectral composition of soil surface.

Many remote sensing techniques are insensitive to nonphotosynthetic vegetation, which can be a major component of total cover in dry ecosystem areas. Spectral mixture analysis (SMA) appears to be the most promising technique to obtain information on vegetation cover, soil surface type and vegetation canopy characteristics. The empirical signature libraries of the world's dominant vegetation types could be upgraded for use with SMA.

Key words: desertification, remote sensing, vegetation, dryland, spectral mixture analysis

2.1 Introduction

The concept of desertification dates back to colonial West Africa in the 1920s and 1930s, and was revived in the early 1970s in an attempt to understand the effects of a long series of drought years that brought environmental degradation, economic difficulty and hunger to the African Sahel (Lonergan, 2005). Many studies and assessments of dryland ecosystems since the United Nations Conference on Desertification (UNCOD) in 1977 have led to a valuable new understanding of the desertification issue. These studies pointed out significant shortcomings in terms of data and methodologies. Moreover, they call for the improvement of science and technology for environmental monitoring, assessment models, accurate databases and integrated information systems (Lonergan, 2005).

Remote sensing is a technology that can be used to measure and monitor important biophysical and biochemical characteristics of objects, as well as human activities on the Earth (Jensen, 2005). The meaning and value of remote sensing data is enhanced through skilled interpretation used in conjunction with conventionally mapped information and ground-collected data (Jensen, 2005). Remote sensing has long been suggested as a time and cost efficient method for observing dryland ecosystem environments (Hassan and Luscombe, 1990).

Optical remote sensing (0.3-15 μm), both spaceborne and airborne, provides valuable tools for evaluating areas subject to desertification. It is used in many applications such as: (1) mapping and monitoring land use and land cover change and degradation, sand dunes, studying organic carbon in the surface soil layer, deriving information about chemical components and mapping areas affected by high salt concentration; (2) studying dryland geomorphology; (3) evaluating the vegetation conditions (e.g. vigour, photosynthetic capacity or stress of vegetation canopy or cluster); (4) studying the atmospheric conditions by detecting mineral aerosols -dust suspended in the air- and water vapour in the atmosphere; (5) detecting the extent of desert (Okin and Robert, 2004).

Earth observation data, particularly Landsat Thematic Mapper (TM) and Multispectral Scanner (MSS) imagery, have been widely used in semiarid environments to show up variations in vegetation community characteristics from changes in their reflectance characteristics. Earth observation data are also used to estimate vegetation abundance depending on simple relationships between reduced reflectance and increased total plant cover or between a spectral vegetation index and green vegetation cover (Pickup, 1995). However, new problems are arising from the changes in vegetation community structure observed in the desert

environment, notably due to a gradual increase in bush dominance and changes in the mix of palatable and unpalatable grasses (Trodd and Dougill, 1998).

This article introduces the reader to the problems of optical remote sensing in studying vegetation in dryland and focuses on: (1) studying the reflectance of vegetation and the surrounding environment in a dryland ecosystem; (2) discussing the techniques used to monitor and obtain information on the canopy in a dryland ecosystem.

2.2 Reflectance of vegetation and surrounding environment in a dryland ecosystem

In the wavelength range between 400 and 2500 nm, the radiance reflected from a vegetation canopy is influenced by three main factors related to the canopy: (1) the optical properties of the vegetation elements, (2) the arrangement of these elements in the vegetation canopy and (3) the optical properties of the environment around the canopy (soil and atmosphere) (Dorigo et al., 2007).

The difficulties facing evaluation of vegetation using optical remote sensing in a dryland ecosystem arise from different types of problems.

2.2.1 Anomalies in the optical properties of the vegetation elements

Vegetation in a dryland ecosystem suffers from water scarcity due to low precipitation and high potential evapotranspiration, so vegetation cover is low. This leads to the small contribution of vegetation reflectance in the total pixel reflectance relative to the other materials in a dryland ecosystem. Therefore, the evaluation of vegetation in a dryland using remote sensing is not completely accurate (White et al., 2000).

The above-mentioned concept has the consequences that the spectral properties of vegetation elements such as stems, leaves and fruits, can be considered the major determinant of canopy reflectance and influence the shape of the overall spectrum (Dorigo et al., 2007). Stems in the dryland ecosystem vegetation, play a small but significant role in determining canopy reflectance in woody plant canopies, especially those with leave area index (LAI) < 5.0. However, this also depends on the location of woody material within the canopy (Asner, 1998). Standing litter significantly affects the reflectance characteristics of grassland canopies.

Furthermore, small increases in the percentage of standing litter lead to unproportional changes in canopy reflectance (Figure 2.1). Variation in litter optical properties plays a secondary role to structural attributes (e.g., leaf and litter area index) in determining canopy reflectance (Asner, 1998).

Regarding the leaves and their reflectance, we can find that they are spectrally dissimilar from their humid counterparts. They have adapted themselves to high temperature and high evaporation losses by adapting their surface in several ways, such as: reducing leaf size, avoiding leaves altogether and moving photosynthesis to the stalks and stem, shading the photosynthetic surface by a high density of reflective spines and leaf hairs or reducing losses due to evapotranspiration by a more waxy leaf cuticle (Ehleringer and Mooney, 1978). These differences affect the overall brightness of dryland vegetation (e.g. creosote – *Larrea tridentata* (DC.) Coville var. *tridentata*), the ratio of green vegetation to nonphotosynthetic vegetation within the canopy and perturbation to the shape of the spectrum at specific wavelengths (Figure 2.2).

Conditions are worsened by the fact that natural plants in arid and semiarid areas coordinate their phenological states with the availability of soil moisture to be able to complete rapidly their reproductive cycle. Persistent vegetation will come out of dormancy when water becomes available after the dry season or a period of drought, begin photosynthesis, and if time permits, produce flowers and fruits. When water again becomes scarce, vegetation will resume dormancy and in an extended period of drought some vegetation will shed their leaves. The total cycle in dryland regions takes place during a relatively short growing season (two to three months). Therefore, no single reflectance spectrum can represent the full spectral phenology of dryland plants, and spectra representing different phenological stages must be incorporated for quantitative information about vegetation change in both space and time (Okin and Robert, 2004).

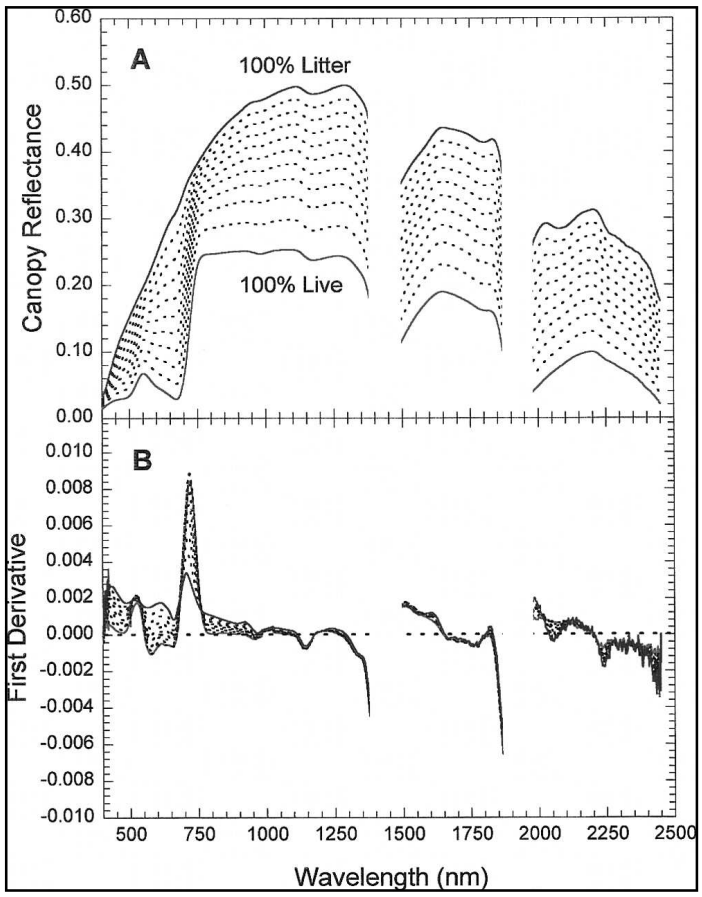

Figure 2.1- A) Effect of increasing the fraction of litter in a grassland canopy from 0% to 100% in simulated canopy reflectance. B) First derivative spectra coinciding with panel A (from Asner, 1998).

The inability of the multispectral data to characterize the vegetation structure can be explained by the limited dimensionality as follows. Scientists have known since 1960 that a direct relationship exists between response in the near-infrared region and variation of vegetation biomass. On the other side, there is a inverse relationship between the vegetation biomass and visible region particularly the red region. To study the structure of the vegetation surface, a plot of near-infrared reflectance versus red reflectance (spectral feature space diagram) was used. At the end of the dry season, in semi-arid areas, bidirectional reflectance values, which are the values of a calibrated reflectance using the sun irradiance geometry function and sensor viewing geometry function, occupy a condensed envelope in spectral space. The pure bush, grass and soil samples lie along a brightness line, which means the red reflectance is equal to

the near-infrared reflectance for pure bush, grass and soil samples (Figure 2.3). This shows the inability of the multispectral data to characterize the vegetation structure. The limited dimensionality means that differences in reflectance between surface component (i. e. grass, bush and soil) are mainly restricted to changes in overall brightness (Trodd and Dougill, 1998).

The disability to provide information on vegetation structure from images acquired during the dry season has a number of important implications regarding the role of satellite imagery in increasing our understanding of vegetation changes in semiarid areas. Particularly, it highlights on the need for long-term ground-based monitoring of changes in vegetation characteristics and data from new satellite sensors in order to help in developing different reflectance models and images analysis for the vegetation community in arid an semi-arid areas. (Ringrose et al., 1989).

2.2.2 Anomalies in the arrangement of elements within the canopy

Most types of dryland vegetation do not differ enough from one another to allow discernment of vegetation types by optical remote sensing (Okin et al., 2001). The within-species variation makes the problem worse as the spectral variability within a species can be greater than the variability between species (Franklin et al., 1993). In order to understand the above mentioned concept, the complication of vegetation community structure and inter-canopy shading are discussed.

Trodd and Dougill (1998) stated that as variations in the relative proportions of bush and grass cover in semiarid zones in Africa are likely to change the composite reflectance, it is apparent that the relationship between vegetation community structure and reflectance is ambiguous. In dryland vegetation community the reduction in reflectance can be due to an increase in vegetation cover and/or inter-canopy shading by bush canopies. Unfortunately, the two effects are not distinguishable and therefore, the relationship between vegetation community structure and reflectance cannot be inverted and used to estimate variations in vegetation structure (Trodd and Dougill, 1998).

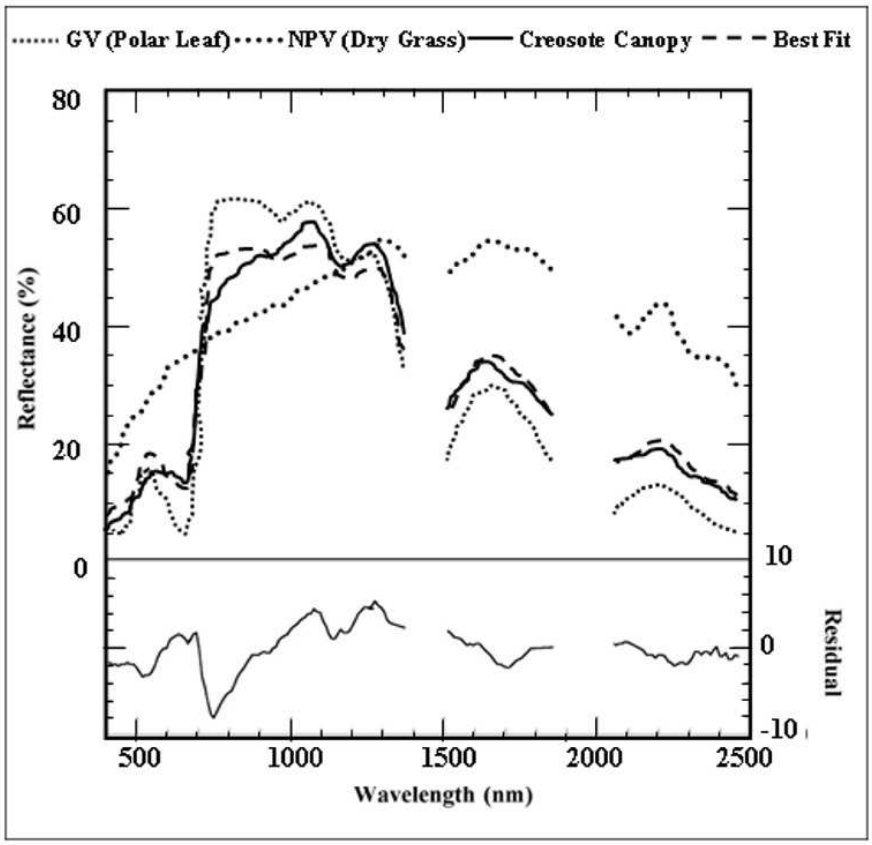

Figure 2.2 - Comparison of green vegetation (GV), nonphotosynthetic vegetation (NPV) and creosote canopy spectra. The best fit line is the optical linear least-squares mixture of GV and NPV to match the creosote spectrum. The residual of this mixture (residual=creosote canopy - best fit) is given in the bottom panel (from Okin and Robert, 2004).

Another important aspect in vegetation community structure in dryland is the possibility of the estimation of the percentage of nonphotosynthetic vegetation (NPV) using remote sensing. NPV whether in the form of dead shrubs or leafless drought-deciduous plants, plays an important role in the environment of dryland regions (Asner, 1998). It is useful in reducing wind and water erosion by contributing to the density of physical obstacles and total surface cover which protect the surface from erosion. Both wind and water erosion occur when surface cover is below approximately 15% (Wiggs et al., 1995). The difficulty is to determine the percentage of NPV and vegetation cover using remote sensing. Many common methods of estimating vegetation cover, such as vegetation indexes, are insensitive to the presence of NPV. They may not be useful to estimate the total cover in situations where NPV is a significant component of the surface cover (Asner, 2004).

2.2.3 Optical interferences from the environment around the canopy (atmosphere and soil)

The most important source of energy is the sun. Before the sun's energy reaches the Earth's surface, three fundamental interactions in the atmosphere are possible: absorption, transmission or scattering. The most efficient absorbers of solar radiation in the atmosphere are ozone, water and carbon dioxide. Atmospheric scattering occurs when the particles or gaseous molecules present in the atmosphere cause the electromagnetic waves to be redirected from their original path (Figure 2.4).

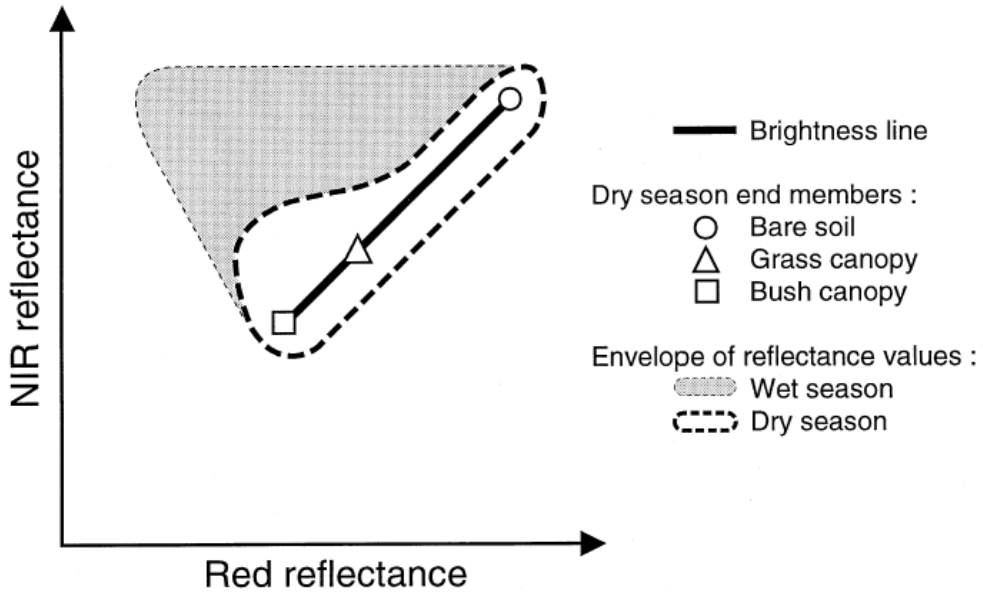

Figure 2.3 - Schematic representation of landscape components in spectral feature space showing the distribution of all pixels in a scene in red and near-infrared multispectural space; the white area envelopes reflectance values in dry season and the white +gray area envelopes reflectance values in the wet season (from Trodd and Dougill, 1998).

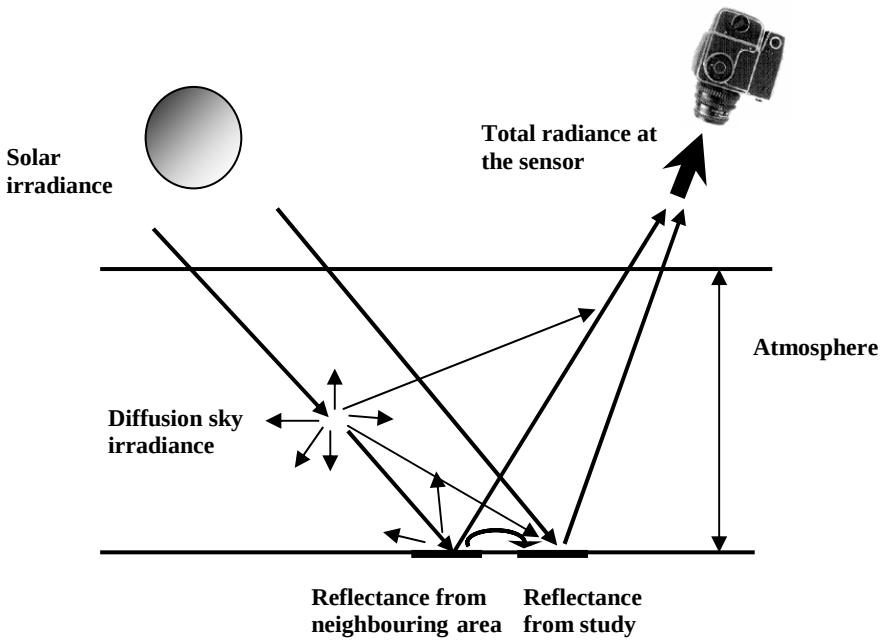

Figure 2.4- Radiance paths from the sun to the sensors: diffusion, scattering and multiscattering.

Simple single scattering is represented as the product of the reflectance of an object times the intensity of the incoming radiation and is called linear mixing. For a given wavelength (λ), we have:

$$I_r(\lambda) = p(\lambda) I_i(\lambda) \qquad [1]$$

where $I_r(\lambda)$ is the intensity of the reflected light, $I_i(\lambda)$ is the intensity of the incident light, and $p(\lambda)$ is the reflectance spectrum of the object.

Multiple scattering or nonlinear mixing occurs when photons interact with more than one type of object on the Earth before returning to the sensor (Asner, 2004) and can be defined as follows:

$$I_r(\lambda) = p_1(\lambda) p_2(\lambda) I_i(\lambda) \qquad [2]$$

where $p_1(\lambda)$ is the reflectance spectrum of the first object and $p_2(\lambda)$ is the reflectance spectrum of the second object.

In arid and semiarid areas where bright soils often underlie vegetation with open canopies, the reflected light is highly affected by this type of multiple scattering. Therefore, correlations of reflected near-infrared radiation with LAI of open canopies of dryland shrubs are poor (Hurcom and Harrison, 1998). Also, in the case of leaf-to-leaf scattering and by referring to the definition of scattering (redirection of the reflectance not reduction), vegetation spectrum in the near-infrared is nonlinearly accentuated. In this case, there is more energy in the near-infrared, therefore, nonlinear mixing is likely to lead to an overestimation of green vegetation cover and an underestimation of shade (Roberts et al., 1993).

In soil, the spectral composition of reflected and emitted energy primarily depends on the biogeochemical (mineral and organic) constituents, optical geometric scattering (particle size, aspect, roughness) and surface moisture (Huete, 2004). Vegetation cover is well correlated with the presence or absence of soil organic matter. Soils in dryland ecosystem areas tend to be bright and mineralogically heterogeneous because of their low organic matter, which tends to mask the spectral contribution of vegetation in individual pixels (Huete and Jackson, 1987).

2.3 Techniques used in optical remote sensing in dryland ecosystems:

Since the launch of the first Earth Resource Technology Satellite (ERTS) on July 23, 1972, the analysis of data has advanced from simple visual observation to sophisticated interpretations based on first principles of spectroscopy and electromagnetic radiation (Ustin et al., 2004). Most remote sensing in arid regions has concentrated on optical remote sensing techniques which use data from sensors that collect radiation in the reflected solar spectrum. Two approaches are usually followed: a) calculation of vegetation indices; b) image classification.

2.3.1 The calculation of vegetation indices

Vegetation indices, reviewed by Jackson et al. (1983), Tueller and Oleson (1989) and others, are generally based on ratios of the radiance in the red and infrared spectral bands, chosen to maximize the reflectance contrasts between vegetation and other materials. The Normalized Difference Vegetation Index (NDVI) has been most commonly used to map spatial and

temporal variation in vegetation (Tucker, 1979). The NDVI is a normalized ratio of NIR and red bands:

$$NDVI = \frac{P_{NIR} - P_{red}}{P_{NIR} + P_{red}} \quad [3]$$

where P_{NIR} and P_{red} are the surface bidirectional reflectance factors.

NDVI is sensitive to pixel-level changes in greenness and fraction of photosynthetically active radiation absorbed, but it is not differentially sensitive to change in vegetation cover versus vegetation condition (i.e. the vigour, photosynthetic capacity or stress of vegetation canopy or cluster). This means that when an NDVI change occurs, it cannot be readily determined whether or not it was caused by altered vegetation cover or condition of cover. Moreover, NDVI has only limited success in providing accurate estimates of shrubland cover in arid regions and limited utility in the arid ecosystem. These facts are due to spectral variability of background materials such as soil and surface litter and the strength and variation of soil spectral albedo (i.e. a pixel may contain reflectance both from vegetation and soil), which causes nonlinearity in the relationship between NDVI and vegetation characteristics (Asner, 2004; Huete, 1988; Huete et al., 1992).

Huete (1988) and Huete et al. (1992) suggested the Soil Adjusted Vegetation Index (SAVI). They introduce a soil calibration factor, *L*, to the NDVI:

$$SAVI = \frac{(1+L)(P_{NIR} - P_{red})}{P_{NIR} + P_{red} + L} \quad [4]$$

where *L* is a soil calibration factor (0-1). Compared to NDVI, SAVI allows to minimize soil background influences.

Regarding the relation between the vegetation indexes and NPV, the role of NPV on NDVI and SAVI was considered by Van Leeuwen and Huete (1996). The significant impact of NPV on these vegetation indexes was demonstrated, but it was so variable as to prevent the formulation

of a single correction algorithm. Certainly, the variability of NDVI of the surface NPV is enormous, and NPV rarely has NDVI values close to zero (Figure 2.5). Therefore, NDVI is difficult to be corrected for instability and ubiquity of NPV surface cover in dryland regions. Due to all these limitations, at the moment, operational guidelines to choose suitable vegetation indices are still lacking.

2.3.2 Image classification

Image classification usually relies on statistical methods including maximum-likelihood, clustering and discrimination analysis (Haralick and Fu, 1983) and methods based on principal components analysis (PCA) (Crist and Cicone, 1984). The aim of image classification is to link image spectra to dominant components in the image captured by the satellite (scene) or a characteristic mixture of components. It is assumed that spectrally similar data will thematically describe similar elements within a scene. It is also assumed that for each pixel there is dominant scene component, or at least a unique and identifiable suite of components that are present in distinctive proportions (Smith et al., 1990a).

PCA is used to identify a change in heterogeneity. To have an accurate measurement, when using this method, the pixel size must be smaller than the scale of variability of at least one of the principle landscape elements (grasslands or shrublands). If the pixel size is greater than the scale of variability, the differences between landscape elements will average out subpixels and spatial information is lost. If it is significantly smaller than the scale of heterogeneity, PCA can be used to examine the distribution of vegetation or soil in a landscape (Phinn et al., 1996).

Spectral mixture analysis (SMA) is a widely used method to unmix the soil-plant canopy measurements into the respective soil, vegetation and NPV single contributions (Smith et al., 1990a). The spectral response in remote sensing from open canopies is a function of the number and type of reflecting components, their optical properties and relative proportions (Adams et al., 1995).

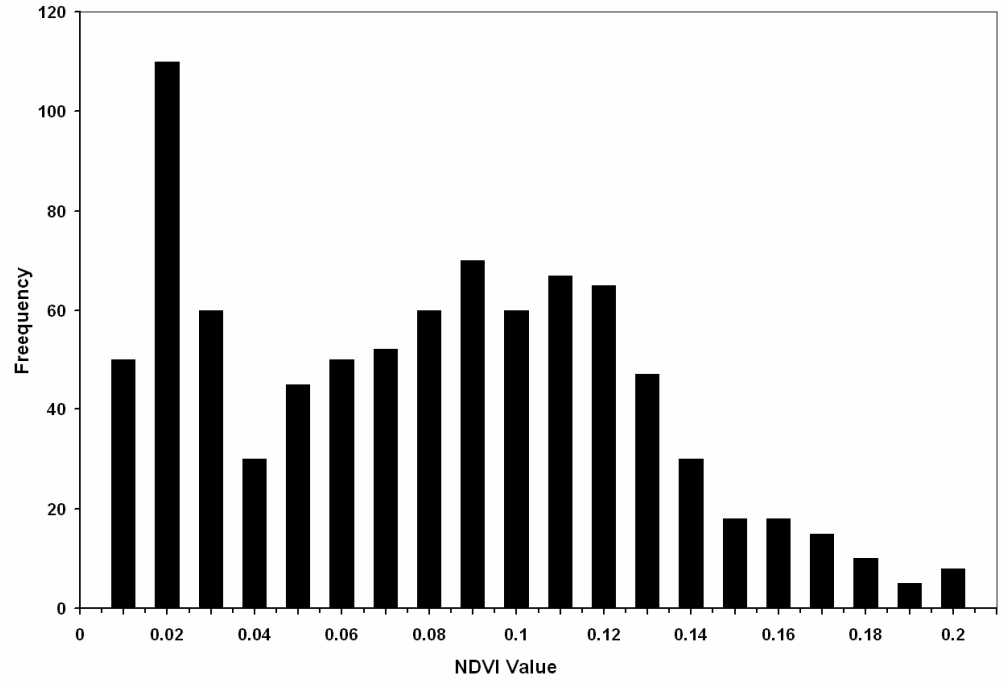

Figure 2.5 - Histogram of NDVI values for nonphotosynthetic vegetation (NPV) collected across a broad range of arid and semiarid ecosystems (n = 972) (from Asner, 2004).

SMA generally involves three steps: 1. assessment of dimensionality or number of unique reflecting materials in a landscape to get the end members; 2. identification of the physical nature of each of the landscape components or endmembers within a pixel; 3. determination of the amounts of each component in each pixel.

The basic SMA equation is:

$$R_P(\lambda) = \sum_{i=1}^{n} f_i R_i(\lambda) + \varepsilon(\lambda) \qquad [5]$$

where $R_P(\lambda)$ is the apparent surface reflectance of a pixel in an image, f_i are the weighting coefficients ($\sum_{i=1}^{n} f_i = 1$) interpreted as fractions of the pixel made up of the endmember i = 1,2 …n, $R_i(\lambda)$ are the reflectance spectra of spectral endmembers in an *n*-endmember model and $\varepsilon(\lambda)$ is the difference between the actual and modelled reflectance.

f_i represents the best fit coefficient that minimizes RMS error (least-squares estimation) given

by the following equation:

$$RMS = \left[\frac{\sum_{j=1}^{m} (\varepsilon_j)^2}{m} \right]^{0.5} \quad [6]$$

where ε_j is the error term for each of the *m* spectral bands considered.

SMA transforms radiation data into fractions of a few dominant endmembers spectra that correspond to scene components. Fraction images illustrate the mixing proportions of these endmembers spectra and therefore, via calibration to field data, the mixing proportions of the scene components can be depicted (Adams et al., 1986; Smith et al., 1985). SMA differs significantly from statistical classification in a number of ways, most significantly in the small number of endmembers compared to the potentially large number of thematic classes required to describe a scene with a statistical approach. Indeed, SMA separates the spectral contribution of these intrinsic scene components from shadow and other effects of illumination. This approach is particularly useful for measuring vegetation cover, especially in dryland regions where the proportions of vegetation and soil may vary significantly over a short distance (Smith et al., 1990a). Spectral mixture models are useful in a variety of applications, including biogeochemical studies, leaf water content, land degradation, land cover conversions, fuelwood assessment and soil and vegetation mapping (Huete, 2004).

Endmembers spectra can be measured in the laboratory, in the field, or from the image itself. Some SMA approaches use endmembers spectra derived from the image (e.g. Wessman et al., 1997; Elmore et al., 2000), whereas others employ libraries of endmembers spectra, which are the empirical signature libraries (e.g. Smith et al., 1990a, b; Roberts et al., 1998). Although in drylands it is exceedingly difficult to locate image pixels containing 100% cover of each appropriate endmember, Bateson and Curtiss (1996) and Bateson et al. (2000) generated SMA model using PCA to explore image data in multiple dimensions. The technique allows the user to select endmember spectra based on inherent spectral variability of the image data without

requiring homogeneous pixels of each endmember. Empirical signature libraries have been used widely, despite the recognition that libraries cannot easily capture the full range of endmember variability as found in nature (Asner, 2004). Indeed, it is unlikely and impractical that the spectral signature of the world's dominant vegetation could be collected given the tens of thousands of species that it would be necessary to identify, and when the range of possible phenological conditions is included, the method becomes impossible. However, the possibility that species and/or communities could be identified by a limited suite of biochemical and architectural characteristics permits new approaches to characterization of land cover properties (Ustin et al., 2004).

Another problem related to the application of SMA is nonlinear mixing, which can hinder the SMA applications (Roberts et al., 1993; Ray and Murray, 1996). However, the importance of the effect is not widely recognised since other studies (Villeneuve et al., 1998; Qin and Gerstl, 2000) showed that nonlinear mixing is a secondary feature. Moreover, Ustin et al., (1986) stated that the role of nonlinear mixing in determining the spectral reflectance variation of an ecosystem is wavelength dependent.

The performance of a spectral mixture model was compared against NDVI for mapping green canopy cover in semi-arid environment using thematic mapper (TM) data by Elmore et al. (2000) (Figure 2.6). NDVI was loosely correlated with green cover but a marked increase in performance was obtained when utilizing the full potential of TM data via spectral mixture analysis (Elmore et al., 2000). Results showed that SMA was able to determine the correct sense of change in percentage live cover and give precise estimates of the magnitude of that change.

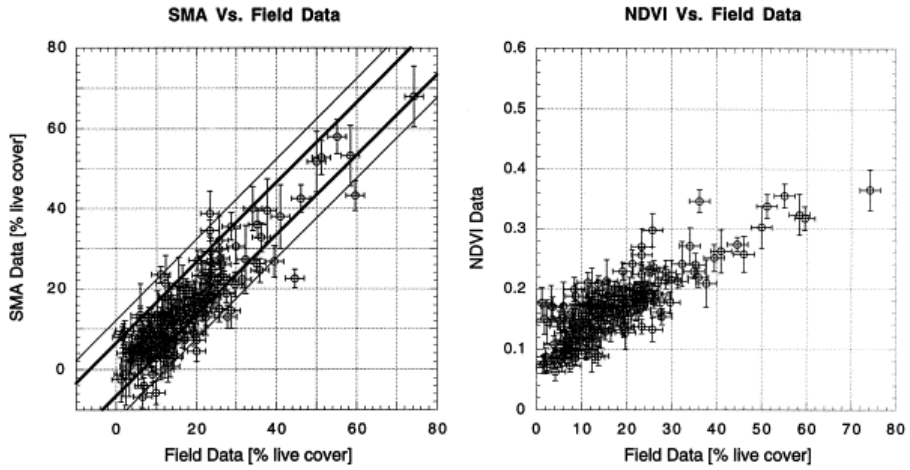

Figure 2.6 - Comparison of subpixel green vegetation cover using Landsat TM imagery collected over a semiarid region: live cover measured in the field (x axis) plotted against (a) SMA results and (b) NDVI (from Elmore et al., 2000).

2.4 Conclusion

Aerial and space remote sensing provide valuable tools for desertification studies, although they must be combined with ground-collected data. From the above review, it is clear that the spectral reflectance of vegetation in arid and semiarid areas changes with the vegetation structure and surrounding environment. To improve our skills in the interpretation of optical remote sensing data in dry ecosystem areas we need increase our understanding of components of these areas (vegetation structure, soil and atmosphere) and develop the techniques of data interpretation. Moreover, the empirical signature libraries should be developed according to regions and environments. The combination of remote sensing and ground-collected data can then provide the basis for the assessment of desertification.

PART THREE:
MONITORING DESERTIFICATION IN A SAVANNA REGION IN SUDAN USING LANDSAT IMAGES AND SPECTRAL MIXTURE ANALYSIS

Dawelbait, M., Morari, F., 2010. Monitoring desertification in a Savanna region in Sudan using LANDSAT images and spectral mixture analysis. Journal of Arid Environment (under reviewing).

Abstract

Two Landsat images, acquired in 1987 and 2008, were analyzed to evaluate desertification processes in central North Kurdufan State (Sudan). Spectral Mixture Analysis (SMA) and multitemporal comparison techniques (change vector analysis) were applied to estimate the long-term desertification/re-growing of vegetation cover over time and in space.

Site-specific interactions between natural processes and human activity played a pivotal role in desertification. Over the last 21 years, desertification significantly prevailed over vegetation re-growth, particularly in areas around rural villages. Changes in land use and mismanagement of natural resources were the main driving factors affecting degradation. More than 120,000 km^2 were estimated as being subjected to a medium-high desertification rate. Conversely, the reforestation measures, adopted by the Government in the last decade and sustained by higher rainfall, resulted in low-medium re-growth conditions over an area of about 20,000 km^2.

Site-specific strategies which take into account the interactions of the driving factors at local scale are thus necessary to combat desertification, avoiding any implementation of untargeted measures. In order to identify the soundest strategies, high-resolution tools must be applied. In this study the application of spectral mixture analysis to Landsat data appeared to be a consistent, accurate and low-cost technique to identify risk areas.

Key words: remote sensing**;** spectral mixture analysis; change vector analysis; Landsat; desertification; savannah.

3.1 Introduction

Desertification is defined as land degradation in arid, semi-arid and dry sub-humid areas due to climate variation and/or human activity (UNCCD, 1994). The three major land use systems prone to desertification in arid and semi-arid areas are rangeland, rain-fed croplands and irrigated lands. Degradation of vegetation cover by overgrazing and the cutting of woody plants for fuelwood, buildings, bush fencing and other purposes are the common desertification processes in rangeland (Mustafa 2007). On rain-fed croplands, wind and water erosion are accelerated by cropland preparation, which involves removal of the native vegetation cover, woodcutting or grass burning. High concentrations of salts in the root zone associated with the introduction of irrigation in dry areas (secondary salinization) have caused desertification due to salts rising with the rise in ground water level (Singh, 2009).

Four aspects must be evaluated in order to render the desertification process measurable (FAO-UNEP, 1984): status, which is defined as the state of a particular piece of land at a specific time compared with its condition in the past; rate, which refers to the change in the condition over time; inherent risk, which is a measure of the vulnerability of landscape to a desertification process; and hazard, which is the overall rating considering the previous three aspects. To make the assessment easier, several Authors have attempted to determine appropriate indicators. Environmental indicators over large areas must be measurable and suitable for regular updating. Few of the proposed indicators are specifically for dryland degradation alone, because it is difficult to separate the effects of climatic factors from those of human activities in such areas (Mabbutt, 1986; Rubio and Bochet, 1998; Diouf and Lambin, 2001).

Difficulties have also arisen because the interpretation of the UNCCD desertification definition can differ greatly according to the choice of indicators. Soil erosion and sedimentation, perennial plant cover and biomass have been used as indicators of the desertification status (Le Houerou, 2006). However a recent survey among 90 experts has recognized the long-lasting loss of vegetation cover and productivity over time and in space as the key indicator/variable of desertification (Hellden, 2008).

One of the most effective tools for desertification assessment is remote sensing. It has long been suggested as a time and cost efficient method for observing dryland ecosystem environments (Hassan and Luscombe, 1990), monitoring land cover degradation, as well as characterizing the dynamism of sand dunes (Collado et al., 2002).

Most remote sensing in arid regions has concentrated on optical remote sensing techniques which use data from sensors that collect radiation in the reflected solar spectrum. Two main approaches are usually followed (Smith et al., 1990a; Dawelbait and Morari, 2008): a) calculation of vegetation indices; b) image classification.

A relationship between plant biomass and a standardized vegetation index can be established (Tucker, 1979). Vegetation indices, reviewed by Jackson et al. (1983), Tueller and Oleson (1989) and others, are generally based on ratios of the radiance in the red and infrared spectral bands, chosen to maximize the reflectance contrasts between vegetation and other materials. The Normalized Difference Vegetation Index (NDVI) has been most commonly used to map spatial and temporal variation in vegetation (Tucker, 1979). NDVI is sensitive to pixel-level changes in greenness and fraction of photosynthetically active radiation absorbed but is not differentially sensitive to change in vegetation cover versus vegetation condition (i.e. the vigour, photosynthetic capacity or stress of vegetation canopy or cluster). This means that when an NDVI change occurs, it cannot be readily determined whether or not it was caused by altered vegetation cover or condition of cover (Asner, 2004). Moreover, NDVI has only limited success in providing accurate estimates of shrubland cover in arid areas and limited utility in an arid ecosystem. This is due to spectral variability of background materials such as soil and surface litter and the strength and variation of soil spectral albedo, which causes nonlinearity in the relationship between NDVI and vegetation characteristics (Huete, 1988; Huete et al., 1992; Asner, 2004).

Image classification usually relies on statistical methods including maximum-likelihood, clustering and discrimination analysis or methods based on principal components analysis (PCA) (Smith et al., 1990a). PCA is used to identify a change in heterogeneity. However, to obtain an accurate measurement the pixel size must be smaller than the scale of variability of at least one of the principle landscape elements (e.g. grasslands).

Spectral mixture analysis (SMA) is a sub-pixel classification technique which could be use to unmix the soil-plant canopy measurements into the respective soil, vegetation, and non-photosynthetic vegetation (Smith et al., 1990a). SMA depends on the spectral response of land cover components. The spectral response in remote sensing from open canopies is a function of the number and type of reflecting components, their optical properties and relative proportions (Adams et al., 1995). SMA appears to be the most efficient technique to obtain information on vegetation cover, soil surface type and vegetation canopy characteristics in semiarid areas

because the scale of variability of the principle landscape elements in semiarid areas is larger than the pixel size in most of the remote sensing satellite imageries (Adams et al., 1995; Okin and Robert, 2004; Dawelbait and Morari, 2008).

Sudan is a developing country where desertification is widespread. UNEP considers that three compounding desertification processes are underway (UNEP, 2007): climate-based conversion of land types from semi-desert to desert, mainly due to a reduction in annual rainfall; degradation of existing desert environments, including wadis and oases, principally caused by deforestation, overgrazing and erosion; conversion of land types from semi-desert to desert by human action (deforestation, overgrazing and cultivation) even if rainfall may still be sufficient to support semi-desert vegetation. These processes are relatively difficult to distinguish, separate and quantify on the ground (Diouf and Lambin, 2001).

Specific studies are therefore necessary in order to define the driving variables affecting the processes and adopt efficient site-specific strategies to combat desertification. Since limited funds are provided to Sudanese research institutions, remote sensing can be a reliable tool to study desertification without incurring high costs (e.g. Ali and Bayoumi, 2004; Dafalla and Casplovics, 2005; Kheiry, 2007).

This paper aimed to a) test the application of SMA to Landsat images as a tool to study the desertification phenomenon and b) individuate and quantify the driving variables influencing land degradation in a savannah region in the central part of Sudan.

3.2 Material and methods

3.2.1 Study site

The study site is located in the north of Umrowaba in North Kordodan State, central Sudan, in the Sahelian eco-climatic zone (between latitude 12°56′35″ and 13°3′49″N and longitude 31°0′51″ and 31°58′51″ E) (Figure 3.1). The climate is semi-arid with annual rainfall ranging from 200 to 750 mm, concentrated during a few summer months (June to September), with a peak in August. Mean annual temperature is about 20 °C, but the daytime temperature can rise as high as 45 °C during summer.

The soil is a Cambric Arenosols (FAO-UNESCO, 1997), coarse sandy, of Aeolian origin with high infiltration rates and inherent low fertility. Sand sheets and sand dunes stabilized by vegetation are the main natural formations. Natural vegetation consists of trees (*Acacias* spp.), bushes and grass, *Aristida pallida* Steud. on crests of dunes, *Eragrostis termula* Tnismert. in the troughs and *Cenchrus biflorus* Roxb., which grows after crop cultivation. Rangeland and rain-fed croplands are the most important land use systems. The main crops are sorghum (*Sorghum vulgare* Pers.), millet (*Panicum miliaceum* L.), sesame (*Sesamum indicum* L.) and watermelon (*Citrullus lanatus* (Thunb.) Matsum & Nakai). The rainy season usually leads to a short growing period followed by a long dry season with a reduction in green vegetation.

3.2.2 Data acquisition and preprocessing

Landsat Thematic Mapper (TM5) and Landsat Enhanced Thematic Mapper plus (ETM+7) scenes acquired on September 15th 1987 (TM5 Sep 15) and October 18th 2008 (ETM+7 Oct 18) were analyzed. The dates coincided with the end of the rainy season when the vegetation biomass was at its highest level. They were selected for monitoring the potential long-term processes of desertification, since both of them were acquired in periods of comparable rainfall amount (4.6 mm in September 1987 and 8.4 mm in October 2008). Landsat images were selected because they are free of charge, with high monitoring frequency and cover areas appropriate for monitoring the environment in a large geographic zone. Landsat TM5 and ETM+7 have a temporal revisit time of 16 days and a spatial resolution of 30 m with six visible/near infrared bands and one thermal band. The gaps in ETM+7 scan-line corrector (SLC)–off were filled using the localized linear histogram mach (LLHM) method (Scaramuzza et al., 2004). Landsat 7 ETM+ SLC - off, November 3rd 2008 was used to fill the gaps since the time lag between the two images was only 15 days and the gaps were not overlapping.

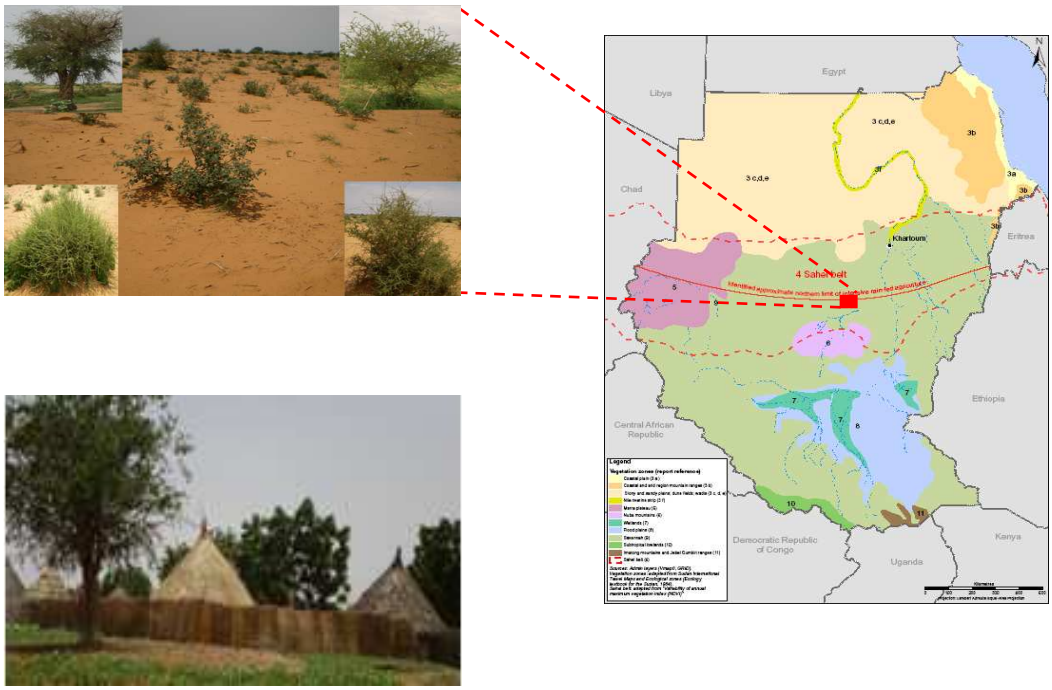

Figure 3.1- Study site position and main landscape elements.

ETM+7 Oct 18 was co-registered to TM5 Sep 15 to undertake comparative analysis. Images were not referenced to a standard map base, since the only available map had a coarser resolution (scale 1:250,000). They were geometrically rectified using 13 ground control points to accurately mach them to ground reference data. The nearest neighbour assignment (Lillesand et al., 2004) was applied yielding a root mean square (RMS) error of 0.34 pixels. Subsets covering only the study area were then extracted from each image. To apply SMA the digital number (DN) of the images band1-5 and 7 recorded in 8 bits were converted to exo-atmospheric reflectance units according to Markham and Barker, (1986). The conversion also improved the image quality (De Asis and Omasa, 2007). No atmospheric correction techniques, such as empirical line calibration (Moran et al., 2001) or dark object subtraction (Chavez, 1988) were applied since they have no significant effect on the modelling (Wu, 2004).

3.2.3 Spectral mixture analysis

In remote sensing images of arid and semi-arid environments, the pixel contains mixed spectral information due to the high variability in the distribution of land cover components. SMA is based on the concept that the variance across a given scene is dominated by the relative proportion of a few spectrally distinct components (Elmore at al., 2000). SMA transforms radiation or reflectance data into fractions of a few dominant endmembers, which are fundamental physical components of the scene and not themselves a mixture of other components (Elmore at al., 2000). Fraction images represent the mixing proportions of these endmember spectra (Smith et al., 1985; Adams et al., 1986). SMA generally involves three steps (Huete, 2004): a) assessment of dimensionality or number of unique reflecting materials in a landscape to obtain the endmembers; b) identification of the physical nature of each endmember within a pixel; c) determination of the amounts of each endmember in each pixel.

The basic linear spectral mixture analysis (LSMA) equation is (Okin and Robert, 2004):

$$R_P(\lambda) = \sum_{i=1}^{n} f_i R_i(\lambda) + \varepsilon(\lambda) \qquad [1]$$

Where $R_p(\lambda)$ is the apparent surface reflectance of a pixel in an image, f_i is the weighting coefficient ($\sum_{i=1}^{n} f_i = 1$) interpreted as fraction of the pixel made up of the endmember i = 1,2 …n, $R_i(\lambda)$ is the reflectance spectrum of spectral endmember in an n-endmember model and $\varepsilon(\lambda)$ is the difference between the actual and modelled reflectance.

fi represents the best fit coefficient that minimizes RMS error given by the following equation:

$$\text{RMS} = \left[\frac{\sum_{j=1}^{m} (\varepsilon_j)^2}{m} \right]^{0.5} \qquad [2]$$

where ε_j is the error term for each of the m spectral bands considered.

One problem related to the application of SMA is nonlinear mixing, which can hinder the SMA

applications (Roberts et al., 1993; Ray and Murray, 1996). Nonlinear mixing occurs when photons interact with more than one type of object on the earth before returning to the sensor (Asner, 2004). However, the importance of the effect is not widely recognised since other studies (Villeneuve et al., 1998; Qin and Gerstl, 2000) showed that nonlinear mixing is a secondary feature.

3.2.4 Endmembers

Some SMA approaches use endmember spectra derived from the image (image endmember) (e.g. Wessman et al., 1997; Elmore et al., 2000), whereas others employ libraries of endmember spectra (library endmember), which are produced from reflectance measurement in a laboratory (e.g. Smith et al., 1990a). Tompkins et al. (1997) pointed out that endmembers selection is the most critical step in SMA to provide a physically meaningful fraction. While library endmembers would undoubtedly represent a purer endmember spectrum and would possibly have given a more accurate absolute abundance, image endmembers simply produce a different scaling and can thus be used for change detection (Elmore et al., 2000). Bateson and Curtiss (1996) and Bateson et al. (2000) generated SMA models using PCA to explore image data in multiple dimensions, although in drylands it is exceedingly difficult to locate image pixels containing 100% cover of each appropriate endmember. One advantage of this technique is that the selection of the endmember spectra is based on inherent spectral variability of the image data without requiring homogeneous pixels of each endmember (Asner, 2004). The approach of Johnson et al. (1985) and Smith et al. (1985) was used to select the endmembers in this paper. The method is based on PCA application to identify the individual endmembers of multiple surface components. The authors observed that for a mixture of three substances (e.g. minerals) the scatter-plot of the first two principle components produced a triangle in which the 'pure' endmembers were located at the corners. Several studies have adapted this technique by analyzing different principal component pairs and have managed to successfully obtain image endmembers within different environments (Drake and White, 1991; Theseira et al., 2003; Brandt and Townsend, 2006). In this study a PCA was applied to Landsat images using ENVI to identify endmembers. The spectral mixing space as represented as orthogonal scatterplots of the first three PC bands were generated and the vertices of these plots were selected as endmembers after visualization in the original images. Endmember spectra were applied to SMA in order to produce the fraction images with associated the RMSE images.

3.2.5 Change detection

Long-term variation in land use and land cover (LULC) was obtained by calculating the difference in fraction images applying map-algebra and Change Vector Analysis (CVA) (Malila, 1980; Kuzera et al., 2005). CVA allows the direction and magnitude of change between two time periods to be evaluated. Vegetation and soil vulnerable to erosion fraction images were used to monitor the vegetation re-growing and desertification between 1987 and 2008. Change direction was measured as the angle of the change vector from a pixel measurement in 1987 to the corresponding pixel in 2008. Angles measured between 90° and 180° indicated an increase in sand and decrease in vegetation, and therefore an increase in desertified area. On the contrary, angles measured between 270° and 360° indicated a decrease in sand and an increase in vegetation and therefore represented re-growth conditions. Angles measured between 0°-90° and 180°-270° indicated either increase or decrease in both vegetation and sand, and consequently persistence in the conditions (Khiry, 2007). Change of magnitude is measured as the Euclidean distance or length of the change vector from a pixel measurement in 1987 to the corresponding pixel in 2008. Four classes of magnitude were represented for either desertification or re-growing according to Kuzera et al. (2005).

3.2.6 Field survey

A 2-weeks field survey was conducted in October 2008 in order to test the accuracy of SMA using ground vegetation data as references. A total of 16 mixed ground cover plots (size 60 x 60m for each plot) were selected. Vegetation was composed of a mixture of acacia trees, bushes, grass and shrubs. Trees and bushes were georeferenced with a GPS and the crown diameters were measured and orthogonally projected to the ground surface to estimate the percentage cover. The percentage cover of grass and shrubs was estimated using the line point intersect sampling method (Elmore at al., 2000). Measurements of the grass and shrubs were taken along 30 60-m long transects, oriented in N-S direction, every 2 m. Measurement points were selected at 60 cm intervals along the transect. The grass and shrubs under the trees and bushes were ignored. The accuracy of SMA was estimated by scatter plot correlation comparing total percentage of live cover in each plot with the live cover (vegetation) fraction image.

3.3 Results and discussion

3.3.1 Endmember spectra and SMA applications

The PC analysis of TM5 Sep 15 data found that the first three components explained over 99% of the variance and that simulated data were mean-corrected and projected onto the space determined by those components. In this PC-reduced space five endmembers were manually selected (Figure 3.2): bright vegetation (BV), dark vegetation (DV), bright soil (BS), dark soil (DS) and non-photosynthetic material (NPM). BV consisted of all types of natural vegetation (e.g. dense shrubs, grass) and cultivated crops with higher leaf chlorophyll and water content. DV consisted of natural vegetation with lower leaf chlorophyll/water content (senescing vegetation). NPM identified villages (e.g. straw houses), dormant trees and senesced grass and shrubs. BS and DS represented coarse sandy soils and fine sandy soils with higher organic matter in the top layer, respectively. A higher soil organic matter content usually also implies a higher soil water holding capacity and subsequently higher water content. The effect of shadow was ignored since it is reduced for the sparse canopies typical of many semiarid bush species (Trodd and Dougill, 1998).

Not all image components can be effectively modelled using simple endmember models (Brandt and Townsend, 2006). The endmember set was selected to maximize the model performance for BV, and BS which is more vulnerable to wind erosion than DS. To find the best quality of fraction images, three combinations of endmembers were tested (Lu and Weng, 2004). The combinations were: 1) all five endmembers; 2) four endmembers with BV, NPM, BS and DS; 3) three endmembers with BV, NPM, and BS. Fraction images derived from different combinations of endmembers were evaluated with visual interpretation, error extent and distribution in the error fraction image. The combination with four endmembers (BV, NPM, BS and DS) was chosen since it provided the best distinction of LULC types and lowest errors.

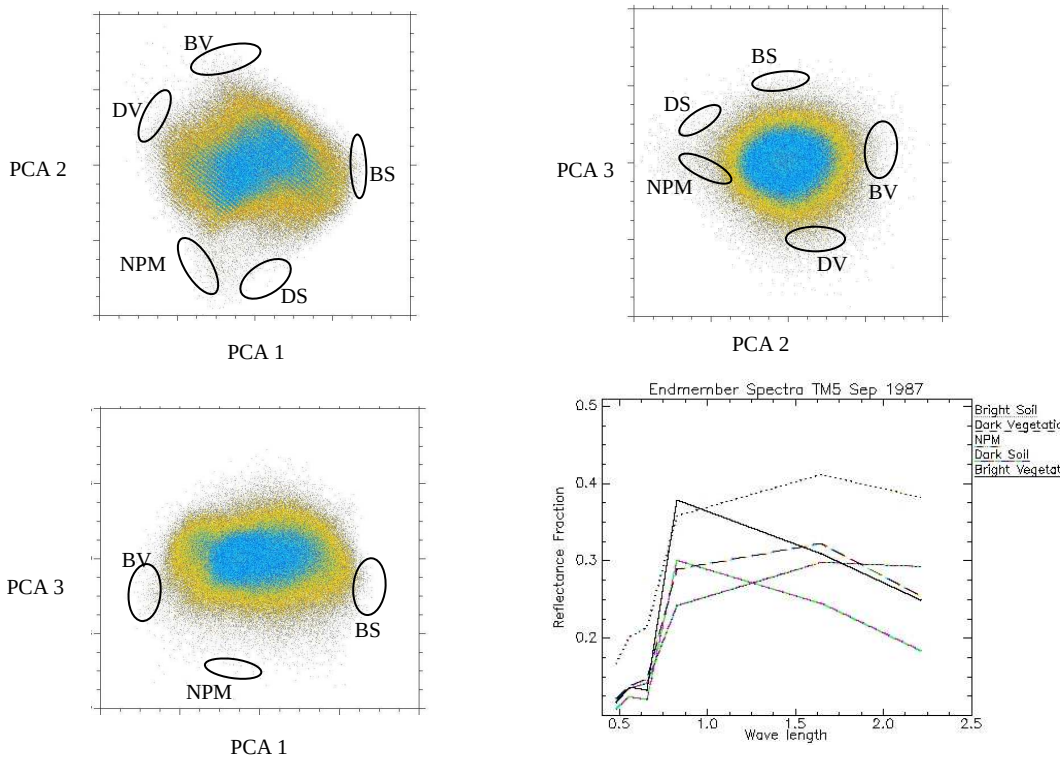

Figure 3.2 - Scatter plot of the first three PCs and location of the five endmembers (a,b,c); endmember spectra (d).

This set of endmember spectra was therefore used across the two selected images. Using the identical endmembers to analyze multitemporal images strengthened the change analysis (Elmore et al., 2000). Similar to using reference endmembers from a spectral library, using identical image endmembers for different images allows a direct comparison of resulting endmember proportions (Brandt and Townsend, 2006). The RMS error images for SMA process ranged from 0% to 3% for TM5 Sep 15, from 0% to 2.9% for TM5 Oct 25 and from 0% to 2.8% for ETM+7 Oct 18.

Figure 3.3 shows the scatter plot correlation between the percentage of vegetation determined with SMA (ETM+7 Oct 18) and field data. In general, the correlation between them is good with an R^2 of 0.91 but with a slight overestimation, especially at lower SMA values. There are three main sources of error that could have affected the comparison. The first one can be due to the misregistration of multidate scene and location of the field sites. This is potentially the largest source of error (Elmore et al., 2000), especially in our case where the geometric rectification was done with 13 ground control points for all the scenes before subsetting of the

study area. This was done because the study area had no fixed sharp points that could be used as control points. Moreover, most of the sites were characterized by a higher degree of scene heterogeneity that could have increased the uncertainty in location (Elmore et al., 2000). Other sources of error can be related to the application LLHM method error to fill the gaps in ETM+7 Oct 18 (Scaramuzza et al., 2004) and accuracy of the field survey, especially in the estimation of grass and bushes. Considering the comparative approach of the present work, the overestimation errors were considered acceptable to evaluate the LULC change.

3.3.2 Change detection

SMA was performed to determine the relative proportions of BV, BS, DS and NPV for each satellite image (Figure 3.4). High abundance of each endmember is indicated in the figures by brighter pixels whereas low abundance is indicated by darker pixels.

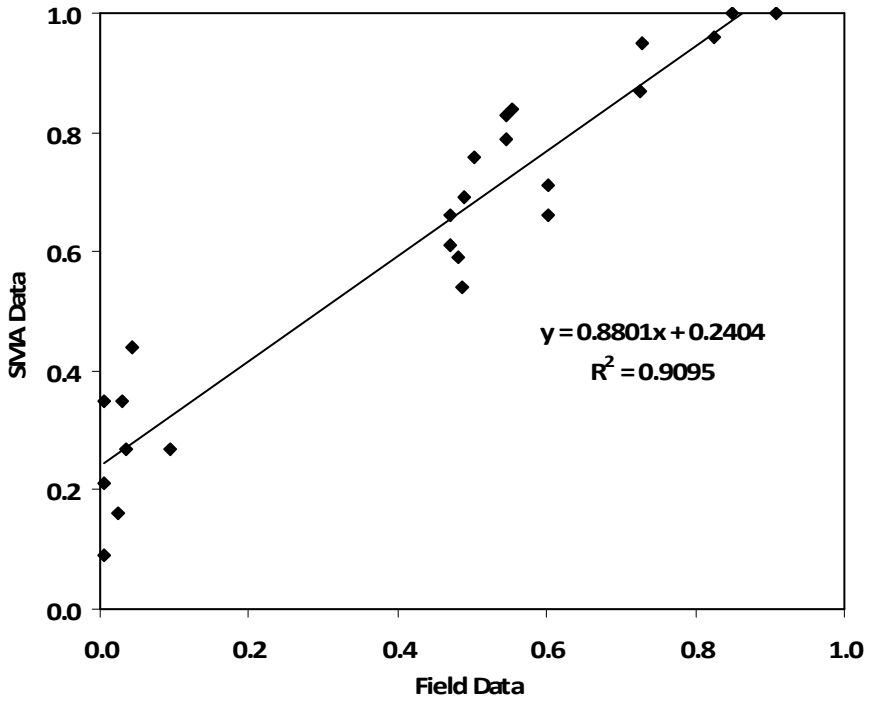

Figure 3.3 - Scatter plot correlation between measured and SMA estimated vegetation fraction in 2008.

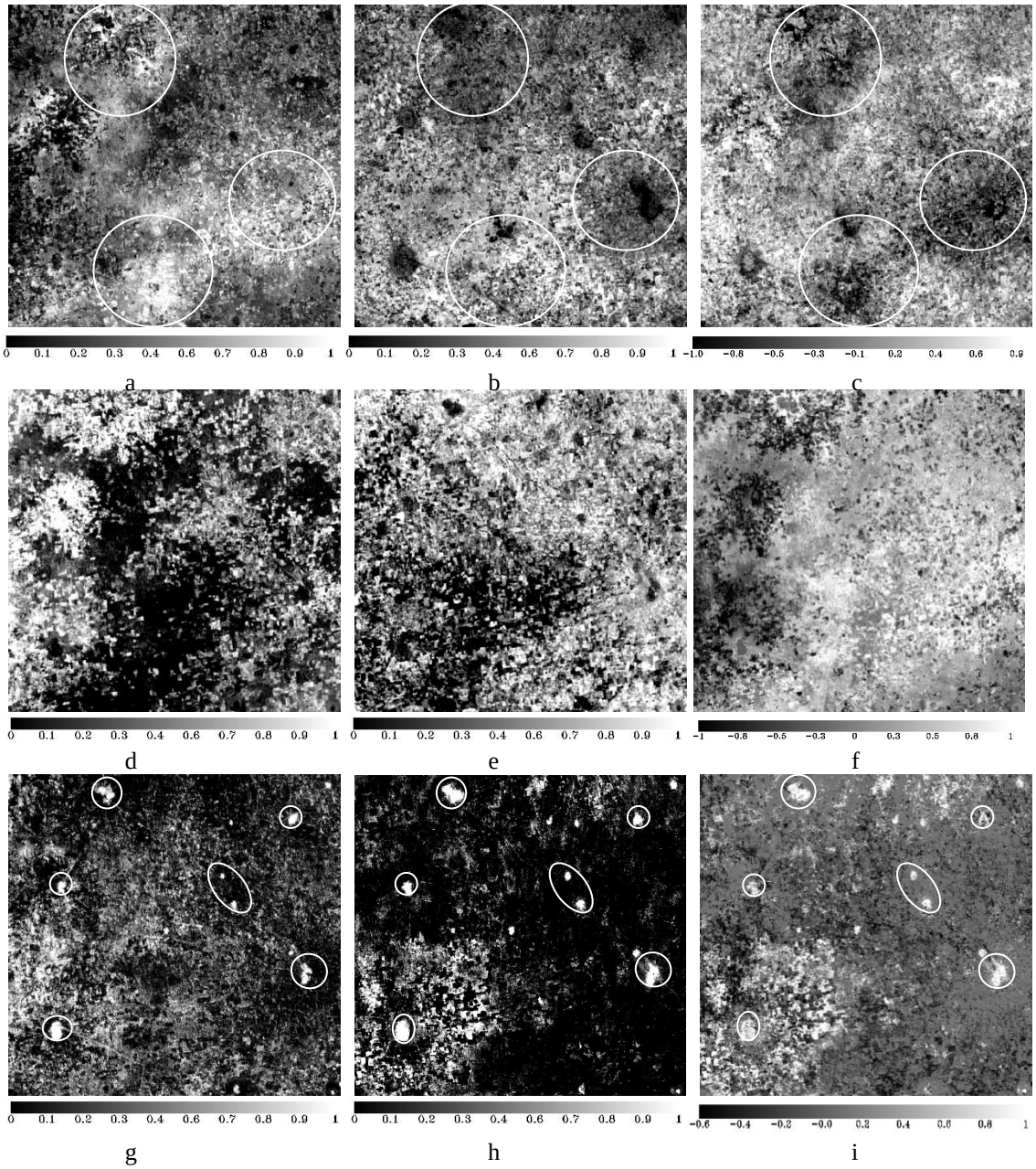

Figure 3.4 - BV, BS and NPM fraction images and change detection in long-term monitoring: (a) BV in 1987, (b) BV in 2008, (c) difference in BV, d) BS in 1987, (e) BS in 2008 (f) difference in BS, (g) NPM in 1987, (h) NPM in 2008 and (i) difference in NPM. Circles in (a), (b) and (c) indicate the three main areas affected by desertification; circles in (g), (h), (i) indicate the rural villages and their expansion over 21 years.

Images analysis clearly indicates the existence of heterogeneous and contrasting conditions within the study site. Relevant negative variations in BV fraction (<-0.1) were observed mainly in three large areas, located near rural villages. In the first two, one in the north and the other in the south, the average change in BV was -0.1 and -0.16 respectively. The eastern part spreads over a larger surface area, with an average change in BV fraction of -0.2.

CVA was quantify desertification processes in degree of severity in (Figure 3.5). The difference in BS fraction for was provided in CVA equation for soil vulnerable to erosion parameter while the difference in BV fraction was substituted for vegetation fractions. According to CVA (Figure 3.5), the magnitude of desertification ranges from low to extreme, with a prevalence of severe degradation conditions (high or extreme) in the eastern part. Change detection analysis also shows the existence of re-growth conditions, mostly spread in the south-western part.

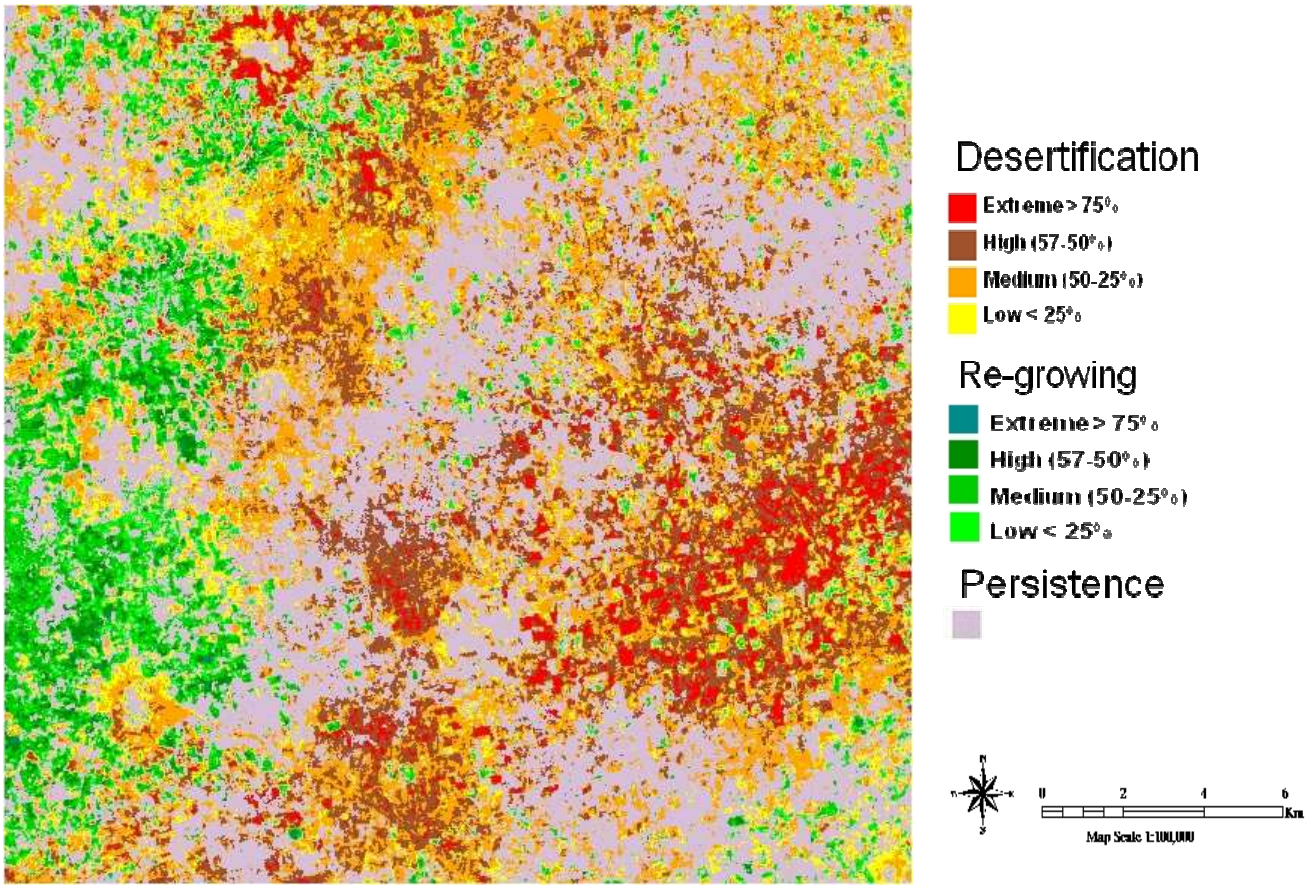

Figure 3.5 - Desertification and re-growth areas calculated by applying change vector analysis.

Overall, desertification prevailed over re-growth, (Figure 3.6) affecting an area of 153,867 km^2, with a prevalence of medium (70,944 km^2) and high (48,578 km^2) classes of magnitude. Re-growth was estimated on an area of 35,313 km^2, mainly classified as medium (17,005 km^2) and low (13,708 km^2). However, average estimation is not sufficient to provide a clear representation of driving factors of change at landscape scale (Collado et al., 2002; Anyamba and Tucker, 2005).

The degradation was driven by various factors, which operated with different intensity in the areas. In the eastern part the expansion of villages triggered the change in land use and mismanagement of the natural resource, mainly caused by deforestation to supply wood for domestic uses i.e. building, cooking, etc., and overgrazing (Sherbinin, 2002). More details of the dynamism around villages are given in Figure 3.7. The NPV fraction change image shows two large patches of pixels with value 1 (new straw houses) due to the expansion of the village over 21 years. In the same area the BV fraction decreases to 0 with a net change of -1, indicating an over-exploitation of the natural vegetation for domestic purposes.

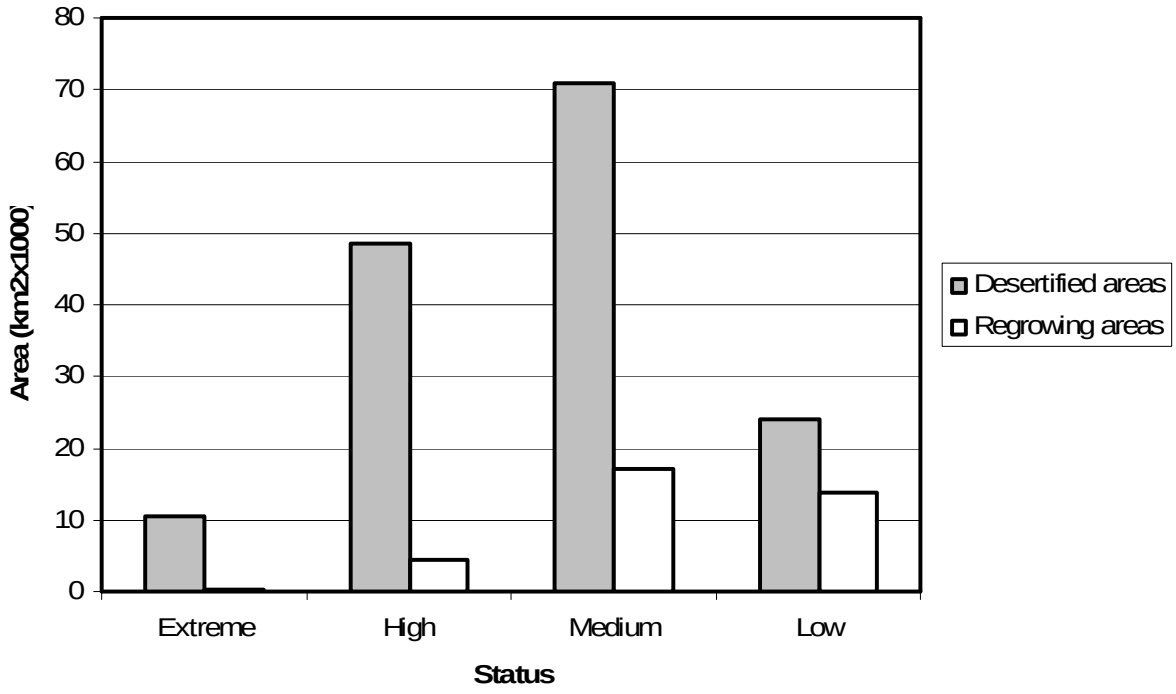

Figure 3.6 - Classification of study site according to the desertification and re-growth magnitude classes.

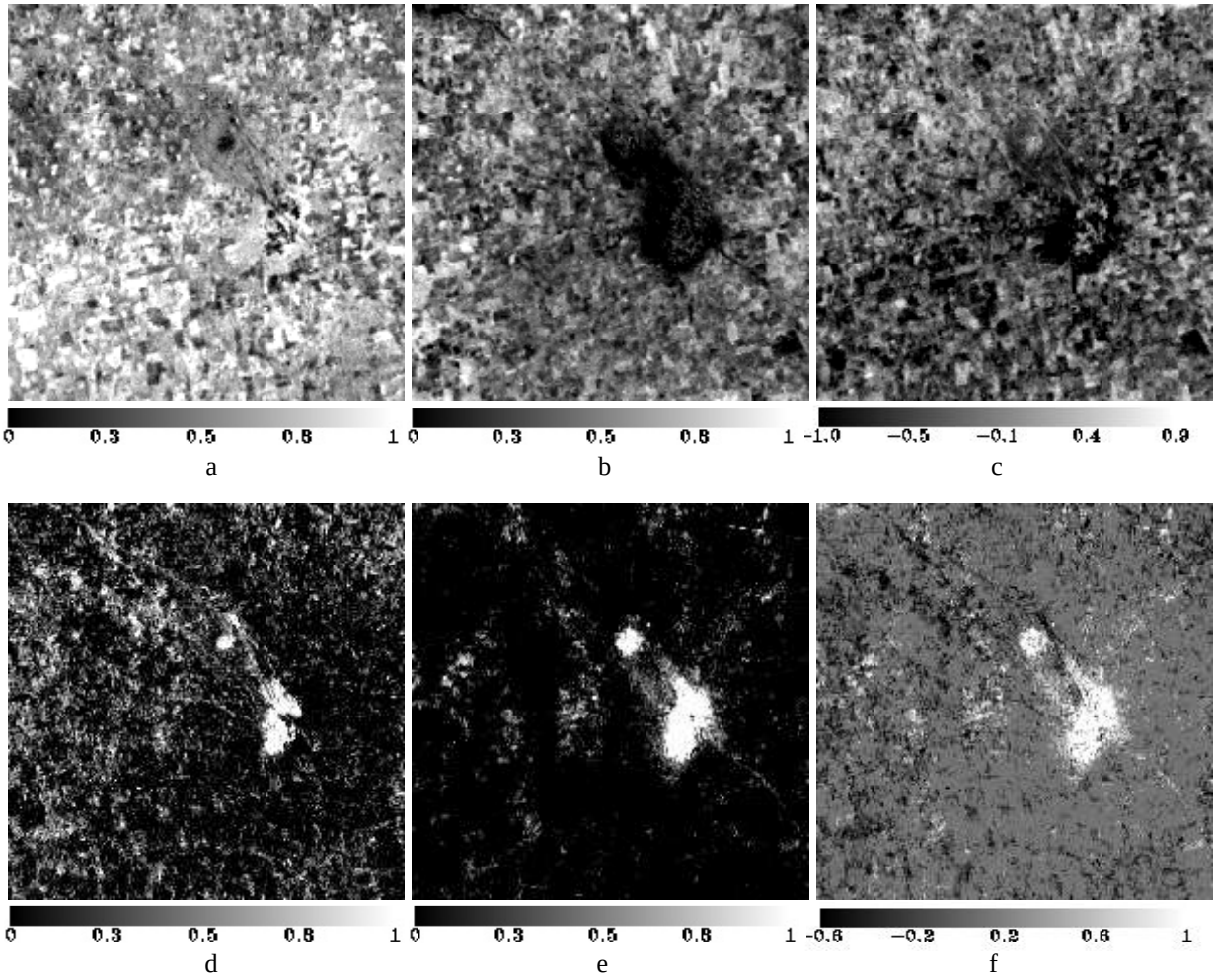

Figure 3.7 - Detailed views of the degraded eastern part of the site: (a) BV in 1987, (b) BV in 2008, (c) difference in BV, (d) NPM in 1987, (e) NPM in 2008 and (f) difference in NPM. The expansion of the village is clearly shown by two large clusters of pixels with value 1 in (f).

Two other processes affecting soil degradation were recognized by SMA. The first one is related to sand encroachment and dune migration, which are considered as one of the main processes of land degradation in arid regions (Balba, 1995). In the northern area a sand dune (locally called Gouz) is visible in the BS fraction image of 1987, along the SE borders of the village of Tafantara (Figure 3.8). At that time, the dune was stabilized by natural vegetation but deforestation for domestic purposes and overgrazing caused the degradation of the site. The change in BV fraction clearly demonstrates the magnitude of the process (Figure 3.8). The degradation led to the encroachment of the sand dune in an E-SE-S direction according to the prevailing wind direction in winter and early summer (Figure 3.8) and consequently the sand fraction in the SE increased in 2008.

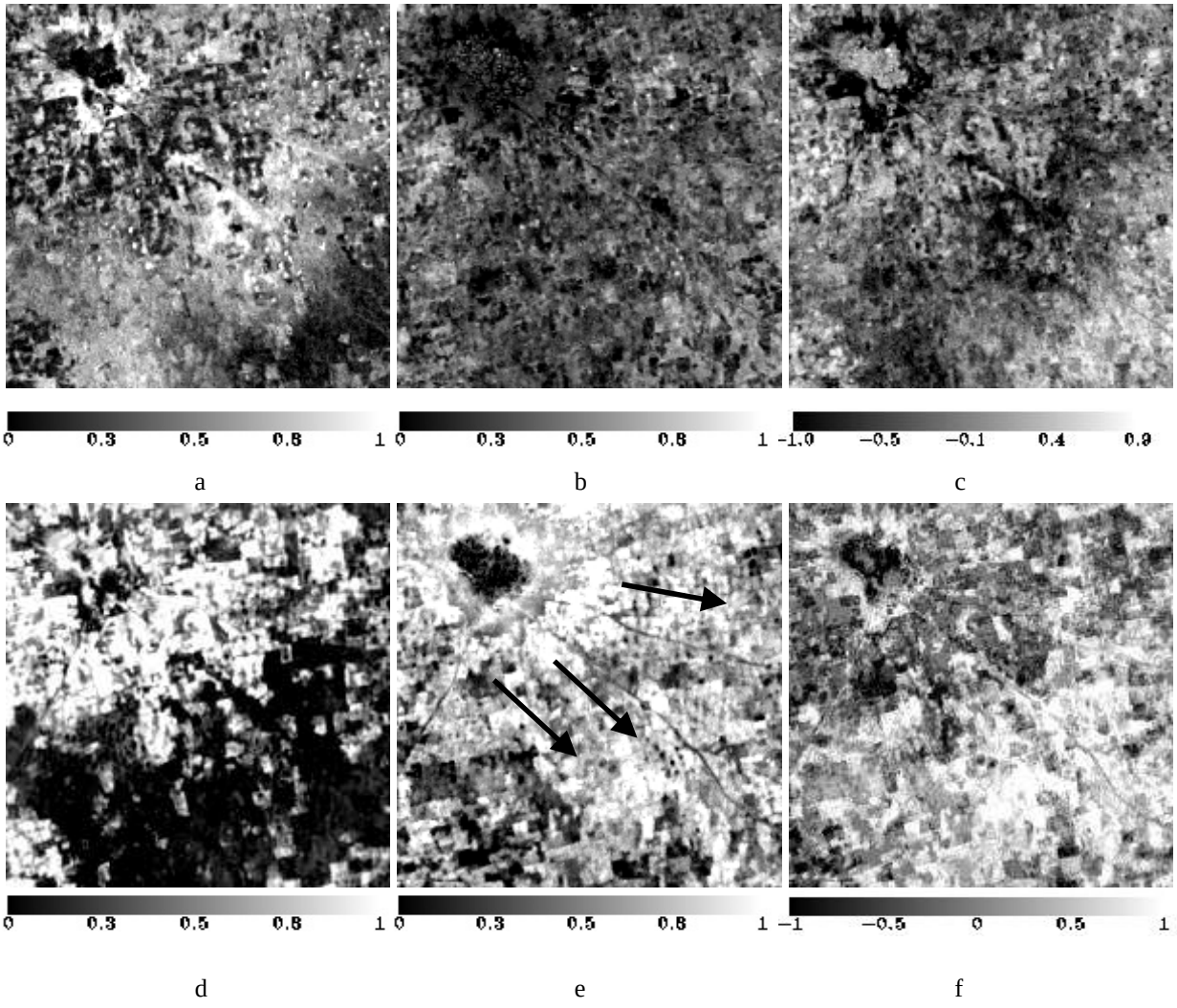

Figure 3.8 - Detailed views of the degraded northern part of the site: (a) BV in 1987, (b) BV in 2008, (c) difference in BV, (d) BS in 1987, (e) BS in 2008 and (f) difference in BS. Figures clearly illustrate the effect of sand movement according to the prevailing wind directions (arrows).

The conversion of rangeland into cultivated croplands is the third phenomenon affecting the desertification of the study site. In the southern part (Figure 3.9), the BV fraction in 1987, on average 0.46, was represented mainly by rangeland. At the same time the average BS fraction was 0.1. The change in land use to cultivation led to a decrease in BV, especially in the central part and a contemporary massive increase in BS fraction. The conversion of dry and fragile rangelands into traditional and mechanized cropland has already been indicated by many Authors as one of the main processes affecting desertification in Sudan. Over-exploitation of semi-desert environments through deforestation, overgrazing and cultivation results in habitat

conversion to desert, even though rainfall may still be sufficient to support semi-desert vegetation (Nicholson, 2005).

Re-growth conditions observed in the SW part were mainly due to Government reforestation projects in last decade and sustained by higher rainfall in the last years in the study area. The Rainfall Anomaly Index (RAI) (Tilahun, 2006) time series (Figure 2.10) confirmed the existence of favourable conditions for vegetation growth from the 1990s to 2008, with higher frequency of positive anomalies than in the 1970s and 1980s.

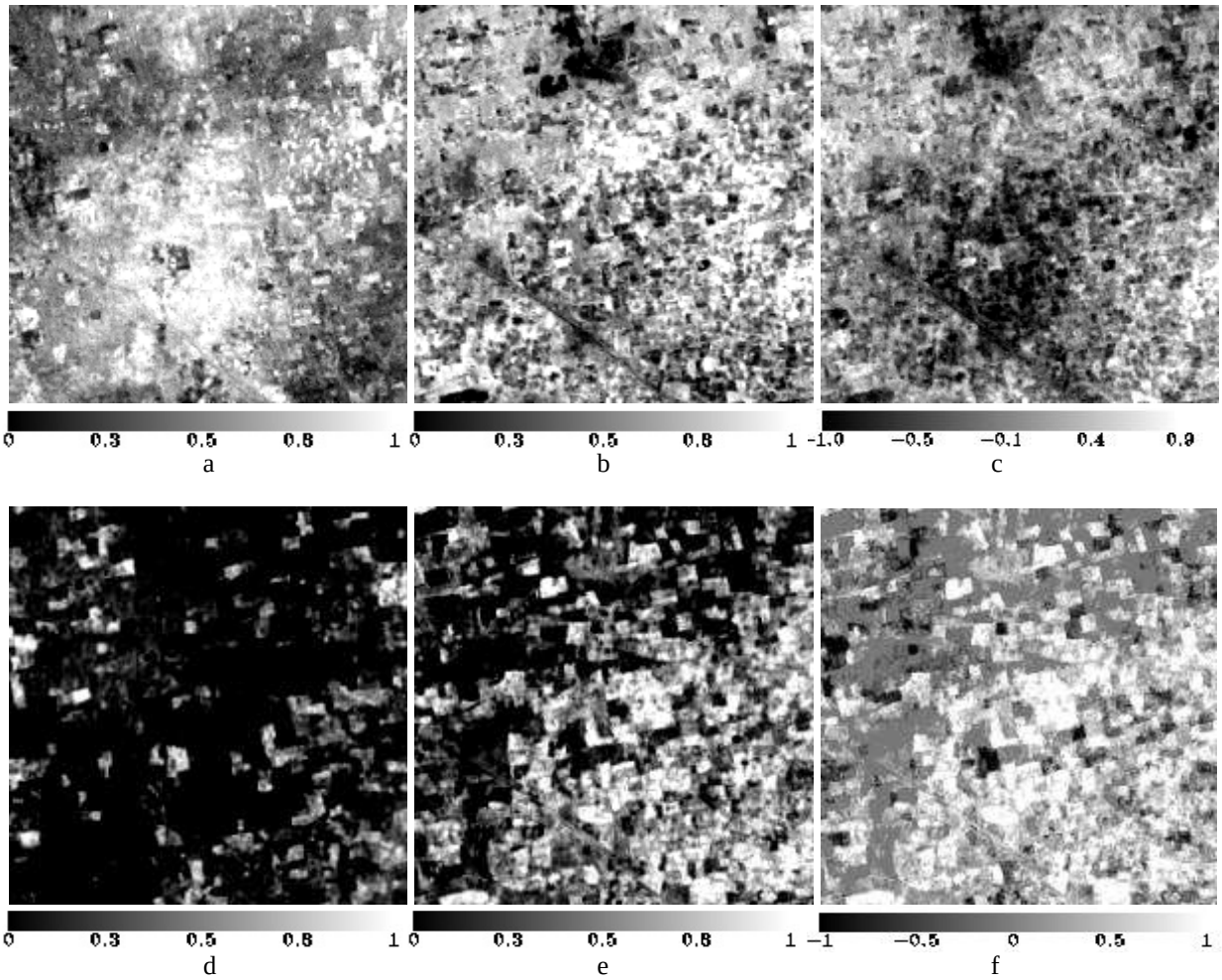

Figure 3.9 - Detailed views of the degraded southern part of the site: (a) BV in 1987, (b) BV in 2008, (c) difference in BV, (d) BS in 1987, (e) BS in 2008 and (f) difference in BS.

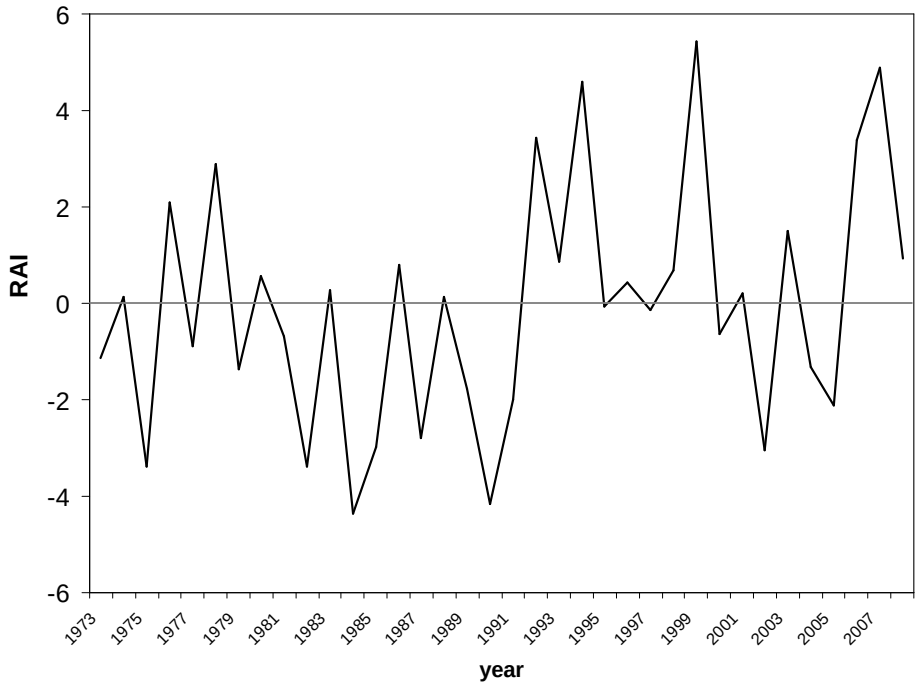

Figure 3.10 - Rainfall Anomaly Index (RAI) from 1973 to 2008.

This result is in accordance with the recent satellite and model based studies of the Sahel (e.g. Eklundh and Olson, 2003; Anyamba and Tucker, 2005), which demonstrated that vegetation has recovered from the peak drought conditions suffered in the region in the 1980s. For example, Anyamba and Tucker (2005), monitoring the Sahelian vegetation dynamics using NDVI in the period 1981-2003, observed the prevalence of greener than normal conditions from the 1990s to 2003. Indeed, NVDI time series followed a similar increase in rainfall over the region during the last decade and indicates a gradual slow but persistent recovery from the 1980s.

3.4 Conclusions

Site-specific interactions between natural processes and human activity play a pivotal role on desertification in North Kordodan State. Even if phenomena at large scale (e.g. positive rainfall trend) in the last years have allowed a gradual recovery from the peak drought conditions suffered in the Sahel during the 1980s, there are still forcing variables that act at local scale to cause land degradation. One of the most important factors affecting such degradation is human activities, which exploit the natural resources beyond their ecological resilience threshold until desertification is irreversible (Hellden, 2008). Hunger and local energy needs seem to be the driver of land use and management.

Site-specific strategies that take into account the interactions of the driving factors at local scale are thus necessary to combat desertification, avoiding the implementation of untargeted measures. In order to identify the soundest strategies, high-resolution tools must be applied. In this study, the application of spectral mixture analysis to Landsat data appeared to be a consistent, accurate and low-cost technique to obtain information on vegetation cover, soil surface type, and identify risk areas.

PART FOUR:
SPATIAL-TEMPORAL ASSESSMENT OF DESERTIFICATION IN THREE DIFFERENT ECOLOGICAL ZONES IN SUDAN 1987-2008

Abstract

Variations in landscape patterns according to the ecological zones play a great role in desertification processes. The amount of vegetation cover, types of dry ecosystem vegetation and structure and phenology of vegetation regarding to the harsh environment differ from one ecological zone to another.

Three Landsat images, acquired in 1987, 1999 and 2008, were analyzed to evaluate desertification processes in three different ecological zones in Sudan (North Kordofan, River Nile and Northern state). Spectral Mixture Analysis (SMA) was adopted using endmembers spectra derived from the images. Multitemporal comparison techniques (visual interpretation and change vector analysis) were applied to estimate the long-term desertification/re-growing and to emphasize land cover variation over time and in space. Site-specific interactions between natural processes, climate variation and human activity played a pivotal role in desertification, however their interaction varied according to the ecological zone.

Different factors drove the desertification in the three areas. In site1, human activities strongly affected degradation phenomenon. The expansion of villages triggered the change in land use and mismanagement of the natural resource, mainly caused by deforestation to supply wood for domestic uses. The degradation moreover promoted sand encroachment and dune migration. In different way climatic constrains drove desertification in sites 2 and 3. Drought, degradation and soil erosion were the causes and effects of desertification. In these sites re-growth conditions were observed only where forestry or agricultural projects were established. Site-specific strategies which take into account the interactions of the driving factors at local scale are thus necessary to combat desertification, avoiding any implementation of untargeted measures.

4.1 Introduction

In the ecosystems prone to desertification, under natural condition, vegetation cover varies from sparse or non-existent in the deserts and arid zone to relatively dense in the wetter parts of the semi-arid regions (Okin and Robert, 2004; Mustafa, 2007). Vegetation is more vulnerable to degradation in drier part of arid region than the wetter part. Degradation of vegetation cover exposes the surface of land and makes it vulnerable to soil erosion (Asner, 2004; Mustafa, 2007).

Arid and semi-arid regions include most of the world's shrub-land, grassland and savannas and support a large fraction of the world's food production, so there is high pressure on land (Graetz, 1994; Asner, 2004). The population growth in this areas cause mismanagement in such fragile area by overgrazing, cutting wood for domestic use and changing land use.

Soil erosion is the main process of desertification and land degradation. Commonly, it is grouped into three phase: (1) physical detachment of soil particles, (2) transportation of soil material by wind and water, and (3) deposition of soil material, including their accumulation and sand dunes (Huete, 2004). Inherent erodibility of the soil, extent of protective ground cover, topography, climate and landuse are factors affecting erosion in arid and semi-arid. Vegetation and soil movement could be processes in desertification as well as factors cause erosion. On rain-fed croplands, wind and water erosion are accelerated by cropland preparation, which involves removal of the native vegetation cover, woodcutting or grass burning (Sherbinin, 2002; Mustafa, 2007).

Wind and water erosion is extensive in many parts of Africa. Excluding the current deserts, which occupy about 46% of the land mass, about 25% of the land is prone to water erosion and about 22% to wind erosion (Reich et al., 2001). High intensities of these erosion forms occur mainly in the semi-arid and sub-humid areas. The soils in Central Africa are largely low activity Oxisols and Ultisols and are less susceptible to water erosion than wind erosion, unless severely mismanaged (Oldeman et al., 1991).

Sudan is one of African countries facing desertification. The arid and semi-arid areas in Sudan cover an area of 1.78 million km^2, which represents about 72% of the total area of the country. Three complex desertification processes are ongoing (UNEP, 2007): climate-based conversion of land types from semi-desert to desert, mainly due to a reduction in annual rainfall; degradation of existing desert environments, including wadis and oases, principally caused by

deforestation, overgrazing and erosion; conversion of land types from semi-desert to desert by human action (deforestation, overgrazing and cultivation) even if rainfall may still be sufficient to support semi-desert vegetation. These processes are relatively difficult to distinguish, separate and quantify on the ground (Diouf and Lambin, 2001; UNEP, 2007).

Regional and national planning to combat desertification can be performed more efficiently if accurate spatial information on the risk of desertification and its evolution in the time are provided. Maps which show such information can be produced through the use of satellite images and digital data and field indicators (Ayoub, 2004). Rozanov (1990) have emphasized the need for developing a system of desertification evaluation by using indicators, such as vegetation and soil change. Remote sensing of vegetation cover and soil is thus critical for regional scale monitoring. In order to use remote sensing in mapping desertification processes study of optical properties of the vegetation and soil elements is needed.

Variations in landscape patterns according to the ecological zones play a great role in desertification processes. The amount of vegetation cover, types of dry ecosystem vegetation and structure and phenology of vegetation regarding to the harsh environment differ from one ecological zone to another. These factors affect the contribution of vegetation reflectance in the total pixel reflectance relative to the other materials (Okin and Robert, 2004; Dawelbait and Morari, 2008). Mineral and organic matter, soil structure and moisture content of the soil surface are the main factors affecting the reflectance of soil in the optical remote sensing.

The meaning and value of remote sensing data are enhanced through skilled interpretation, in conjunction with conventionally mapped information and ground-collected data. Spectral Mixture Analysis (SMA) has proved to be a powerful technique to monitor land cover degradation in arid and semi-arid areas. SMA is a sub-pixel classification technique which could be use to unmix the soil-plant canopy measurements into the respective soil, vegetation, and non-photosynthetic vegetation (Smith et al., 1990a).

Using SMA and LANDSAT images, this study aimed to indentify the main variables driving degradation across three different ecological zones in Sudan and evaluate the desertification risk and its evolution in the time.

4.2 Material and Methods

4.2.1 Study sites

The methods were implemented according to sequence steps and processes given in the flow chart shown in Figure 4.1. Three sites were selected in order to compare processes driving desertification in three different ecological zones: savannah, semi-desert and desert (Figure 4.2).

Site 1 is a flat area located in north of Ummruaba in North Kurdufan State (12°56′35″-13°3′49″N and 31°0′51″-31°58′51″E). Site 2 is located near Aldamer in River Nile State, along the west side of the river Nile (17°29′09″-17°35′41″N and 33°47′03″-33°53′48″E). The landscape is characterized by small valleys oriented in WE direction with seasonal streams. Site 3 is located along the upstream of Waddi Almugadam which runs from the east to the west during the rainy season in Northern State (17°29′10″-18°05′36″N and 31°29′48″-31°36′39″E) (Figure 4.2).

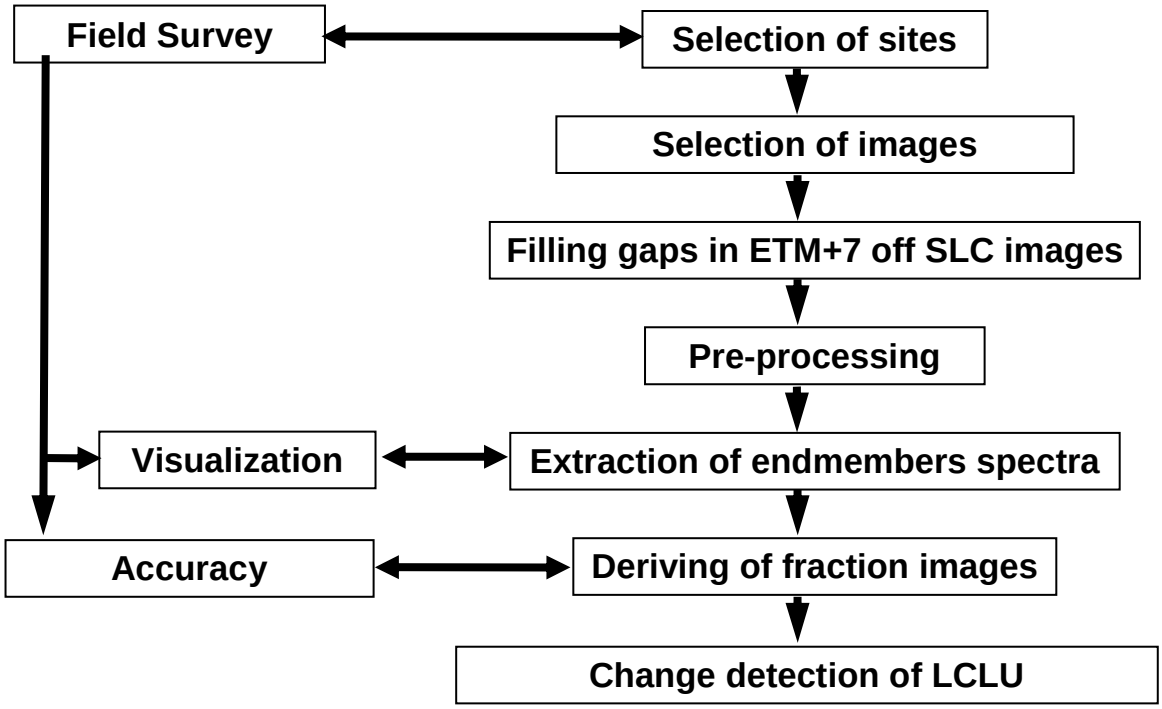

Figure 4.1- Flow chart of the methodology steps and processes.

The vegetation in the three sites is mainly composed by dominant trees, shrubs, grass and in site 1 crops. Natural vegetation in site 1 consists of trees (*Acacias* spp.), bushes and grass, *Aristida pallida* Steud. on crests of dunes, *Eragrostis termula* Tnismert. in the troughs and *Cenchrus biflorus* Roxb., which grows after crop cultivation. Rangeland and rain-fed croplands are the most important land use systems. The main crops are sorghum (*Sorghum vulgare* Pers.), millet (*Panicum miliaceum* L.), sesame (*Sesamum indicum* L.) and watermelon (*Citrullus lanatus* (Thunb.) Matsum & Nakai). Dominant and endogenous trees site 2 are *Capparis decidus* Forsk. and *Acacia ehrenbergiana* Hayne., while *Prosopis chilensis* (Molina) Stuntz. *and Prosopis juliflora* (Sw.) DC. are exotic and invasive. *Acacia seyal* Del., *Leptadenia pyrotechnica* Forssk., *Faidherbia albida* Del. and *Balanites aegyptiaca* (L.) Del. are the dominant trees and shrubs in site 3. More details about ecological zones, climate and soil of the three sites are given in Table 4.1.

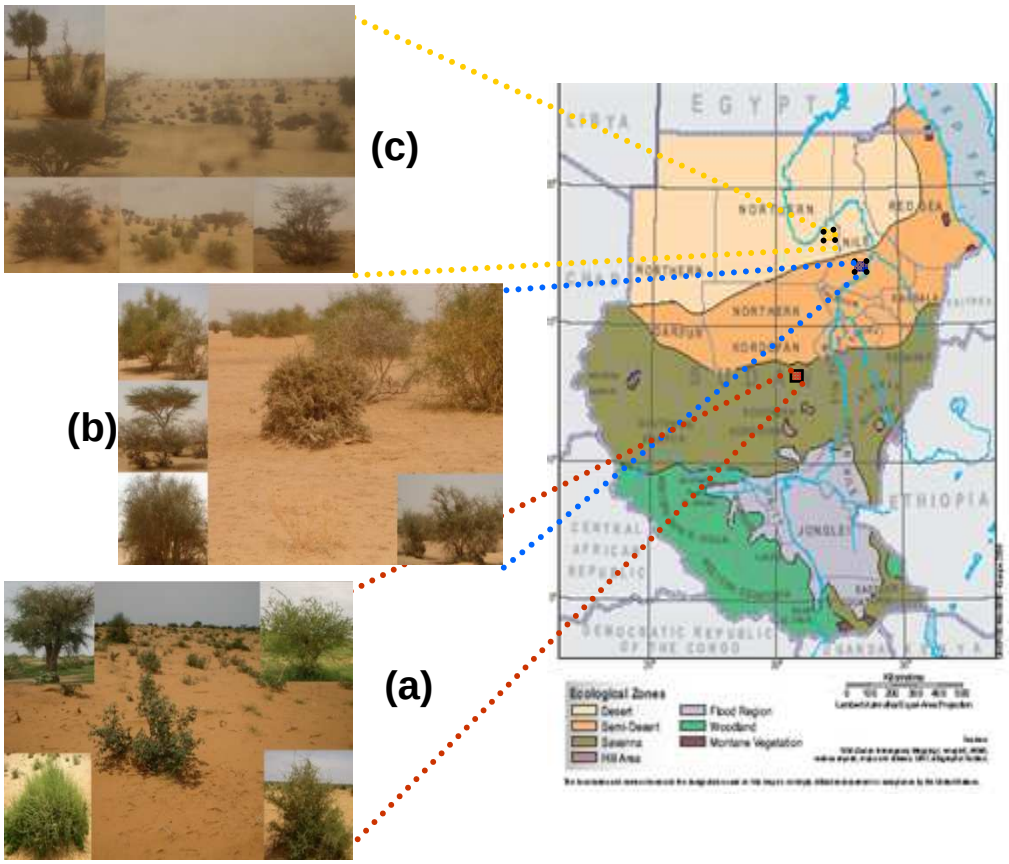

Figure 4.2- Location and landscapes of the three study sites a) site 1 in savanna b) site 2 in semi-desert region c) site 3 in desert region.

Table 4.1- Climate and soils in the three study sites.

	Ecological zone (Harrison and Jackson, 1958)	Annual Precipitation	Temperature in winter °C	Temperature in summer °C	Type of soil (FAO-UNESCO, 1997)
Site 1	Savannah	200 to 750 mm	Mean 13 Min. 10 Max. 25	Mean 27 Min. 20 Max. 45	Cambric Arenosols
Site 2	Semi-desert	50 to 60 mm.	Mean 18 Min. 8 Max. 31	Mean 34 Min. 22 Max. 48	Arenosols, Fluvisols and Cambisols
Site 3	Desert	> 60 mm	Mean 13 Min. 4 Max. 26	Mean 36 Min. 24 Max. 49	Arenosols and Fluvisols

4.2.2 Data acquisition and preprocessing

Three Landsat images were selected and analyzed to study the desertification processes in the three study sites: One Landsat Thematic Mapper (TM5) scene in 1987 and two Landsat Enhanced Thematic Mapper plus (ETM+7 SLC-on) scene in 1999 and (ETM+7 SLC–off) scene in 2008. Times of acquisition of these images are given in Table 4.2. The dates of the images were coincided with the end of the rainy season when the vegetation biomass was at its highest level. While TM5 1987 and ETM+7 SLC-off 2008 were acquired in periods of comparable rainfall amount, ETM+7 SLC-on 1999 images were selected to study the effect of rain. Indeed the mean annual rainfall in 1999 was 581 mm, 162 mm and 83 mm in site 1, 2 and 3 respectively, relativity higher than the mean annual rainfall (Table 4.1). Landsat images were selected because they are free of charge, with high monitoring frequency and cover areas appropriate for monitoring the environment in a large geographic zone. Landsat TM5 and ETM+7 have a temporal revisit time of 16 days and a spatial resolution of 30 m with six visible/near infrared bands and one thermal band. The gaps in ETM+7 SLC-off were filled using the localized linear histogram mach (LLHM) method (Scaramuzza et al., 2004). Landsat ETM+7 SLC-off, November 3rd 2008, October 11th 2008 and October 2nd 2008 were used to fill the gaps in selected ETM+7 SLC-off 2008 images in site 1, 2 and 3 respectively, since the gaps were not overlapping and the time lag between the two images was only 15 days in site 1 and 2 and one month in site 3.

Table 4.2- Acquisition dates of Landsat images.

	1987	**1999**	**2008**
Site1	TM5 - Sep 15th	ETM+7 ON-SLC - Nov 11th	ETM+7 OFF-SLC - Oct 18th
Site2	TM5 - Sep 24th	ETM+7 ON-SLC - Oct 3rd	ETM+7 OFF-SLC - Sep 25th
Site3	TM5 - Oct 01st	ETM+7 ON-SLC - Oct 26th	ETM+7 OFF-SLC - Aug 31st

For each site, the images were co-registered to TM5 to undertake comparative analysis. Images were not referenced to a standard map base, since the only available map had a coarser resolution (scale 1:250,000). They were geometrically rectified using 13, 16 and 14 ground control points in site 1, 2 and 3respectivly to accurately mach them to ground reference data. The nearest neighbour assignment (Lillesand et al., 2004) was applied yielding a root mean square (RMS) error of 0.34, 0.67 and 0.58 pixels in the 3 study sites with consequent order. Subsets covering only the study area were then extracted from each image for each site. To apply SMA the digital number (DN) of the images band1-5 and 7 recorded in 8 bits were converted to exo-atmospheric reflectance units according to Markham and Barker, (1986). The conversion also improved the image quality (De Asis and Omasa, 2007). No atmospheric correction techniques, such as empirical line calibration (Moran et al., 2001) or dark object subtraction (Chavez, 1988) were applied since they have no significant effect on the modelling (Wu, 2004).

4.2.3 Mapping of land cover

SMA appears to be the most efficient technique to obtain information on vegetation cover, soil surface type and vegetation canopy characteristics in semiarid areas. SMA was used in this study to map the land cover. SMA transforms radiation or reflectance data into fractions of a few dominant endmembers, which are fundamental physical components of the scene and not themselves a mixture of other components (Elmore at al., 2000). The basic linear spectral mixture analysis (LSMA) equation is (Okin and Robert, 2004):

$$R_P(\lambda) = \sum_{i=1}^{n} f_i R_i(\lambda) + \varepsilon(\lambda) \qquad [1]$$

Where $R_p(\lambda)$ is the apparent surface reflectance of a pixel in an image, f_i is the weighting

coefficient ($\sum_{i=1}^{n} f_i = 1$) interpreted as fraction of the pixel made up of the endmember *i* = 1,2 …*n*, $R_i(\lambda)$ is the reflectance spectrum of spectral endmember in an *n*-endmember model and $\varepsilon(\lambda)$ is the difference between the actual and modelled reflectance.

fi represents the best fit coefficient that minimizes RMS error given by the following equation:

$$\text{RMS} = \left[\frac{\sum_{j=1}^{m} (\varepsilon_j)^2}{m} \right]^{0.5} \qquad [2]$$

where ε_j is the error term for each of the *m* spectral bands considered.

The most critical step in SMA and production of fractions image is the selection of endmembers. The derivation of the endmembers spectra could be either from the image (image endmember) (e.g. Wessman et al., 1997; Elmore et al., 2000) or measure in laboratory (library endmember) (e.g. Smith et al., 1990a). In this study, endmembers were selected from the images using the approach of Johnson et al. (1985) and Smith et al. (1985). The method is based on PCA application to identify the individual endmembers of multiple surface components. PCA was applied to Landsat images using ENVI to identify the endmembers for each site individually. The spectral mixing space as represented as orthogonal scatter plots of the first three PC bands were generated and the vertices of these plots were selected as endmembers after visualization in the original images. Endmember spectra were applied to SMA in order to produce the fraction images (proportions of endmember spectra) with associated the RMSE images (Smith et al., 1985; Adams et al., 1986).

The problem of nonlinear mixing, which can hinder the SMA applications (Roberts et al., 1993; Ray and Murray, 1996), was ignored since other studies (Villeneuve et al., 1998; Qin and Gerstl, 2000) showed that nonlinear mixing is a secondary feature. More details on SMA application are given in Dawelbait and Morari (2010).

4.2.4 Change detection

Change can be identified explicitly either as change in the number of endmembers or as a change in endmember fractions (Adams *et al.*, 1995). In the study the change analysis was estimated according to the second approach since an identical endmembers set was used to derive fraction images (Elmore et al., 2000). Three approaches was conducted to evaluate the variation in land use and land cover (LULC). The first two focused on visual interpretation of the land cover elements in the different years and direct measument using map-algebra. Visual interpretation for each endmember was performed using a standard RGB composite by displaying fractions images of the three years 1987, 1999 and 2008 as blue green and red, respectively. The third approach consisted in Change Vector Analysis (CVA) (Malila, 1980). CVA allows the direction and magnitude of change between two time periods to be evaluated. The vegetation and soil vulnerable to erosion fraction images were used to monitor the vegetation re-growing and desertification between 1987 and 2008 only since the two years has a comparable amount of rain as main before. Change direction was measured as the angle of the change vector from a pixel measurement in 1987 to the corresponding pixel in 2008. Angles measured between 90° and 180° indicated an increase in sand and decrease in vegetation, and therefore an increase in desertified area. On the contrary, angles measured between 270° and 360° indicated a decrease in sand and an increase in vegetation and therefore represented re-growth conditions. Angles measured between 0°-90° and 180°-270° indicated either increase or decrease in both vegetation and sand, and consequently persistence in the conditions (Khiry, 2007). Change of magnitude is measured as the Euclidean distance or length of the change vector from a pixel measurement in 1987 to the corresponding pixel in 2008. Four classes of magnitude were represented for either desertification or re-grow according to Kuzera et al. (2005).

4.2.5 Field survey

A field survey was conducted during six weeks in late summer 2008 (September-October) in order to test the accuracy of SMA using ground vegetation data as references. In site 1 field survey was conducted in an area located around a group of villages where the effects of human activities in a savannah region could be tested. Abuslaim forest and a cropped area, where a new agricultural projected is ongoing since 2007, were selected in sites 2 and 3 respectively.

A total of 16 mixed ground cover plots (size 60 x 60m for each plot) were selected in each site. Vegetation in the selected plots in all sites was composed of a mixture of acacia trees and bushes. Site 1 only had grass and shrubs in addition. Trees and bushes were georeferenced with a GPS and the crown diameters were measured and orthogonally projected to the ground surface to estimate the percentage cover. The percentage cover of grass and shrubs in site 1 was estimated using the line point intersect sampling method (Elmore at al., 2000). Measurements of the grass and shrubs were taken along 30 60-m long transects, oriented in N-S direction, every 2 m. Measurement points were selected at 60 cm intervals along the transect. The grass and shrubs under the trees and bushes were ignored. The accuracy of SMA was estimated by scatter plot correlation comparing total percentage of live cover in each plot with the live cover (vegetation) fraction image.

4.3 Results and discussion

4.3.1 Endmember spectra and SMA applications

The first three components of PC of TM5 data for each site explained over 99% of the variance and estimated data were mean-corrected and projected onto the space determined by those components. From these PC scatter plots, five endmembers were manually selected in site 1 while three endmembers were selected in site 2 and 3 (Figure 4.3). Two type of vegetation in site 1, bright vegetation (BV1) and dark vegetation (DV1), and one type of vegetation in site 2 and 3 (V2 and V3) were selected. BV1 consisted of all types of natural vegetation (e.g. dense shrubs, grass) and cultivated crops with higher leaf chlorophyll and water content. DV1 consisted of natural vegetation with lower leaf chlorophyll/water content (senescing vegetation). V2 and V3 represented all types of natural vegetation (e.g. dense shrubs, grass). The reflectance of BV1 spectrum at 0.83 micrometer (Band 4) is higher than that in V2 and V3 spectra (Figure 4.4) which indicate higher leaf chlorophyll and water content, while DV1 spectrum is similar to V2 spectrum. The reflectance of V3 spectrum at 0.66 micrometer (band 3) is higher than the reflectance at 0.56 micrometer (band 2) which indicates very low leaf chlorophyll/water content even during the rainy season (Asner, 2004) (Figure 4.4).

Two types of soils were identified in each site. Bright soil (BS1) and dark soil (DS1) in site 1 represented coarse sandy soils and fine sandy soils with higher organic matter in the top layer, respectively. Both BS1 and DS1 absorbed more energy at 2.215 micrometer (band 7) than at 1.65 micrometer (band 5) which indicates availability of moisture content (Jensen, 2005) (Figure 4.4). A higher soil organic matter content usually also implies a higher soil water holding capacity and subsequently higher water content. In site 2 and 3 bright soil (BS2 and BS3) represented Arenosols and Fluvisols soils (coarse sandy soils). Dark soil in site 2 (DS2) represented Cambisols soils (very fine brown soil particles). Both BS2 and DS2 were in dry condition since there was high reflectance in band 7 (Jensen, 2005). The reflectance in Band 5 and 7 of BS3 was the highest one across the three sites. Dark soil in site 3 (DS3) represented coarse and fine sandy soil with relatively high moisture content (Figure 4.4).

Non-photosynthetic material (NPM1) was identified only in site 1. NPM1 represented villages (e.g. straw houses), dormant trees and senesced grass and shrubs. The effect of shadow was ignored since it is reduced for the sparse canopies typical of many semiarid bush species (Trodd and Dougill, 1998).

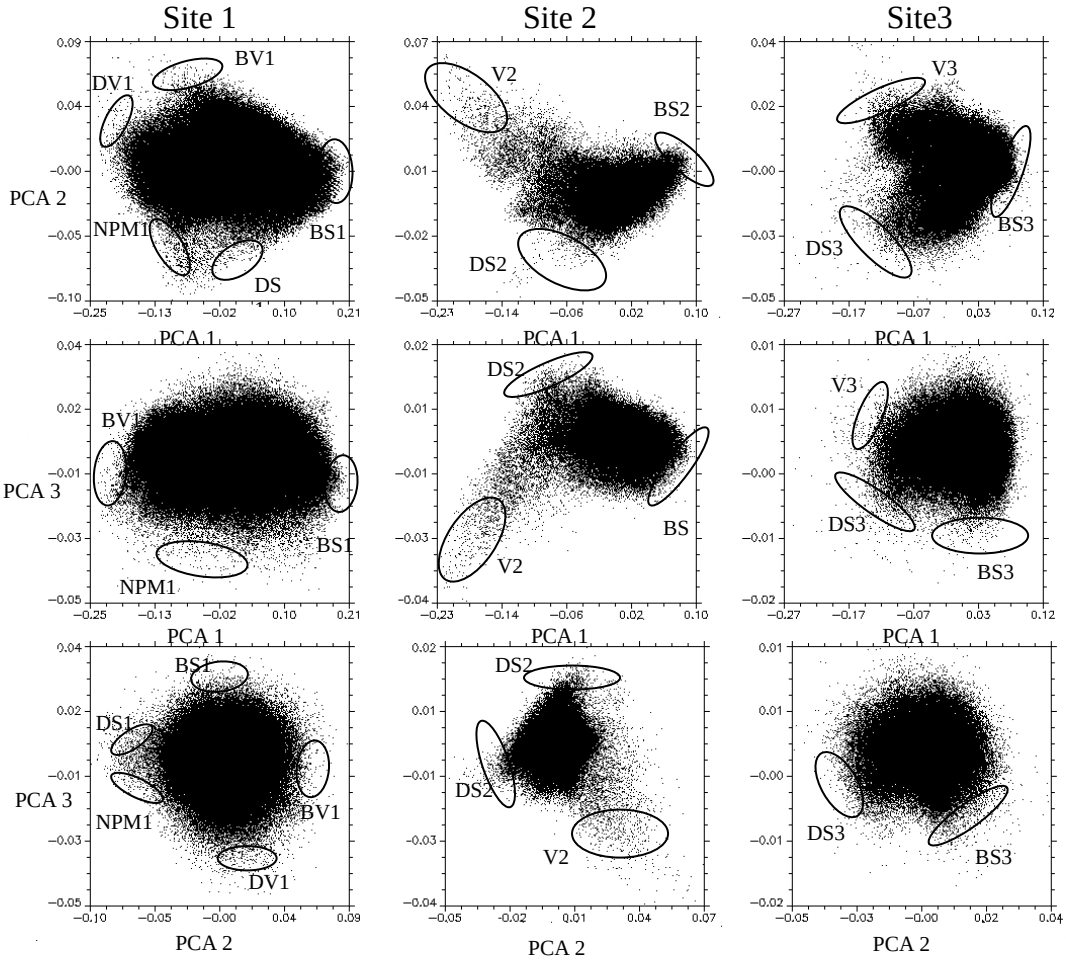

Figure 4.3 - Scatter plot of the three PCs, endmembers location for each site individually.

While BS1, BS2 and BS3 are vulnerable to erosion, DS1 and DS3 are less vulnerable to erosion since moisture content is a resistance factor to soil erosion. On the contrary DS2 is seriously vulnerable to wind erosion because it is drier than the other two dark soils.

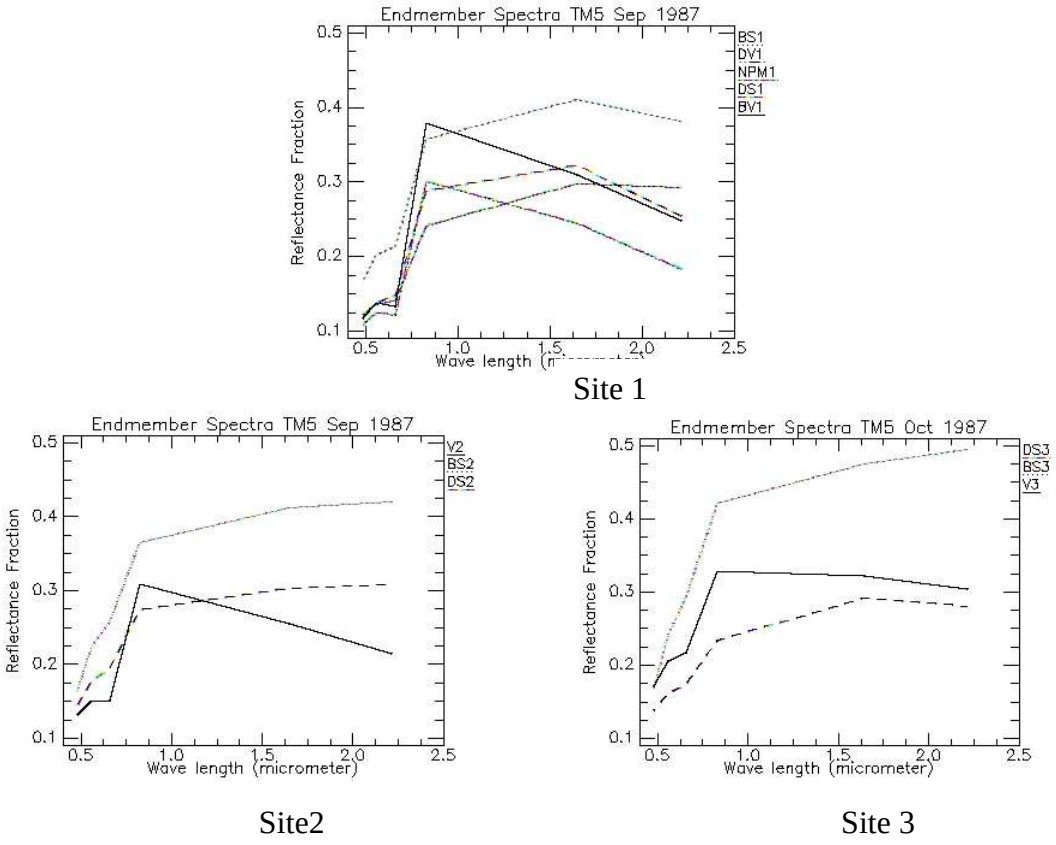

Figure 4.4 - Endmembers spectra for each site individually.

Endmemebers in the three sites were chosen not only according to the observations in the field survey, but also to maximize the model performance and to minimize RMS error (Table 4.3). Accordingly, only four endmembers (BV1, BS1, DS1 and NPM1) from site 1 were selected for applying the fraction images. Relatively high errors were observed in 2008 (Table 4.3) and could be due to the correction of ETM+7 off SLC (Scaramuzza et al., 2004). Figure 4.5 shows the scatter plot correlation between the vegetation fraction estimated with SMA (ETM+7 2008) and measured in the field. In general, the correlation between them is good with an R^2 of 0.75 but with a slight overestimation. Larger discrepancies were observed in site 2.

There are main sources of error that could have affected the comparison. The first one can be due to the misregistration of multidate scene and location of the field sites (Elmore et al., 2000). Other sources of error can be related to the application LLHM method error to fill the gaps in ETM+7 Oct 18 (Scaramuzza et al., 2004) which produced high RMS errors in SMA, especially for site 2, and accuracy of the field survey. Anyway, considering the comparative

approach of the present work, the overestimation errors were considered acceptable to evaluate the LULC change.

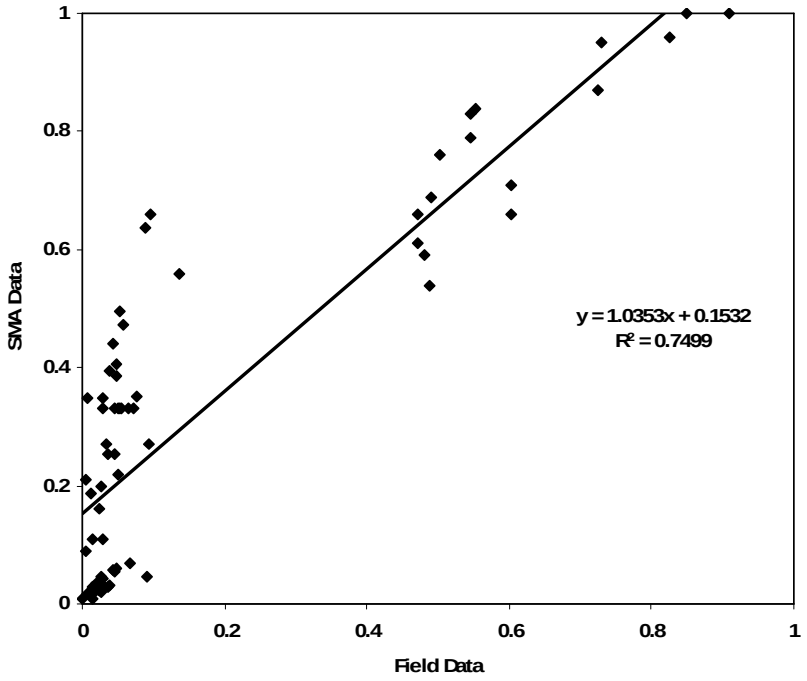

Figure 4.5 - Scatter plot correlation between measured and SMA estimated vegetation fraction in 2008 for the three sites.

Table 4.3 - RMS errors in the application of SMA.

	TM5 - 1987	**ETM+ 7 SLC on - 1999**	**ETM+ 7 SLC off - 2008**
site 1	0% to 3%	0 % to 1.5%	0% to 2.8%
site 2	0% to 1%	0% to 1.8%	0% to 4.6%
site 3	0% to 1%	0% to 1.6%	0% to 4.2%

4.3.2 Change detection

Average estimation of endmember fractions for the three sites are given in Figure 4.6. The effect of the rainfall was very clear for BV (site 1), whose fraction increased of 16% from 1987 to 1999 (the rainiest year) and then decreased in 2008 to the initial level. The same phenomenon was observed also for V2 but not for V3. The fraction of bright soil increased over the 21 yrs in sites 1 (+14%) and 3 (+16%), while in site 2 decreased of 26%. At the same time DS2 increased from 44% to 80%. However, average estimation is not sufficient to provide a clear representation of driving factors of change at landscape scale (Collado et al., 2002; Anyamba and Tucker, 2005).

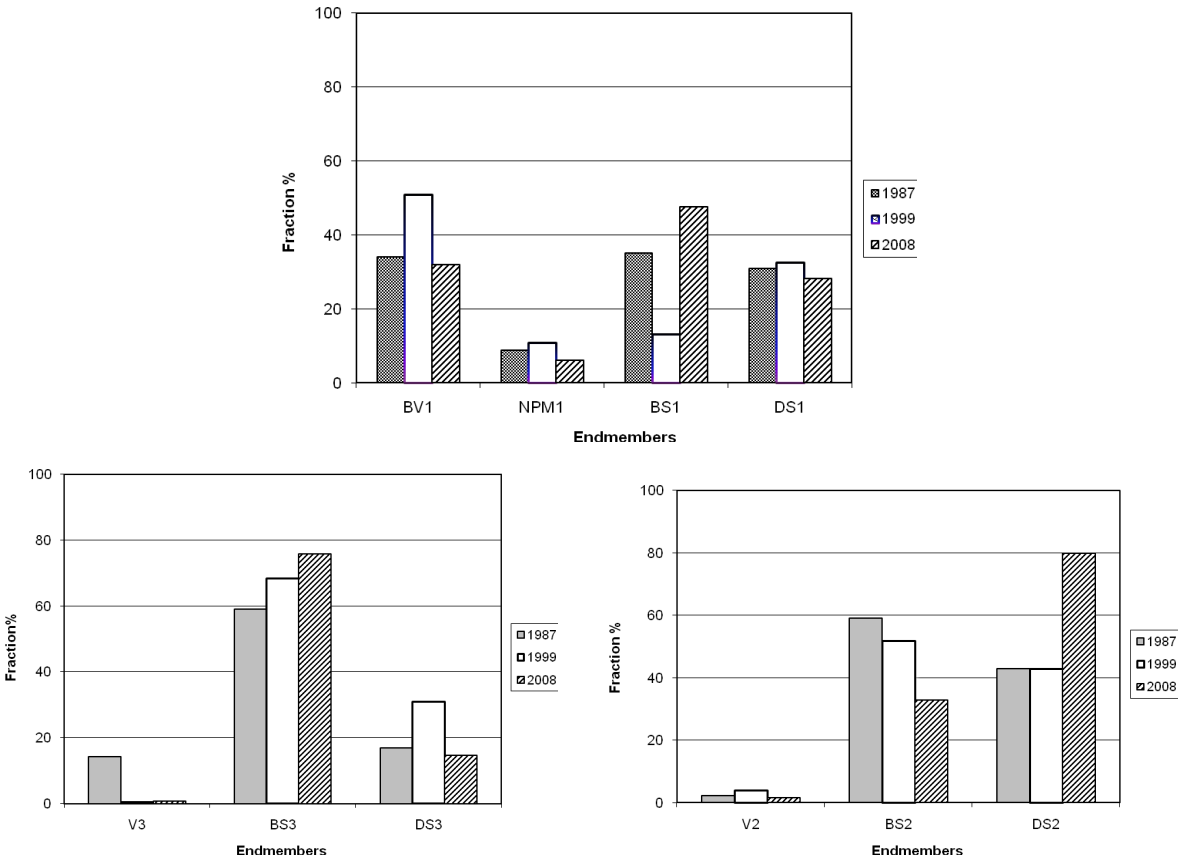

Figure 4.6 - Average estimation of endmember fractions for each site individually.

Tempo-spatial variations of the endmember fractions are visually interpreted by displaying fractions for year 1987 in blue, year 1999 in green and year 2008 in red for each endmember (Figure 4.7). The visual interpretation of color composite shows that the major changes have the most saturated colors while the minor changes have less saturated colors. White tones indicate no temporal change and grey tones indicated no existence for that endmember.

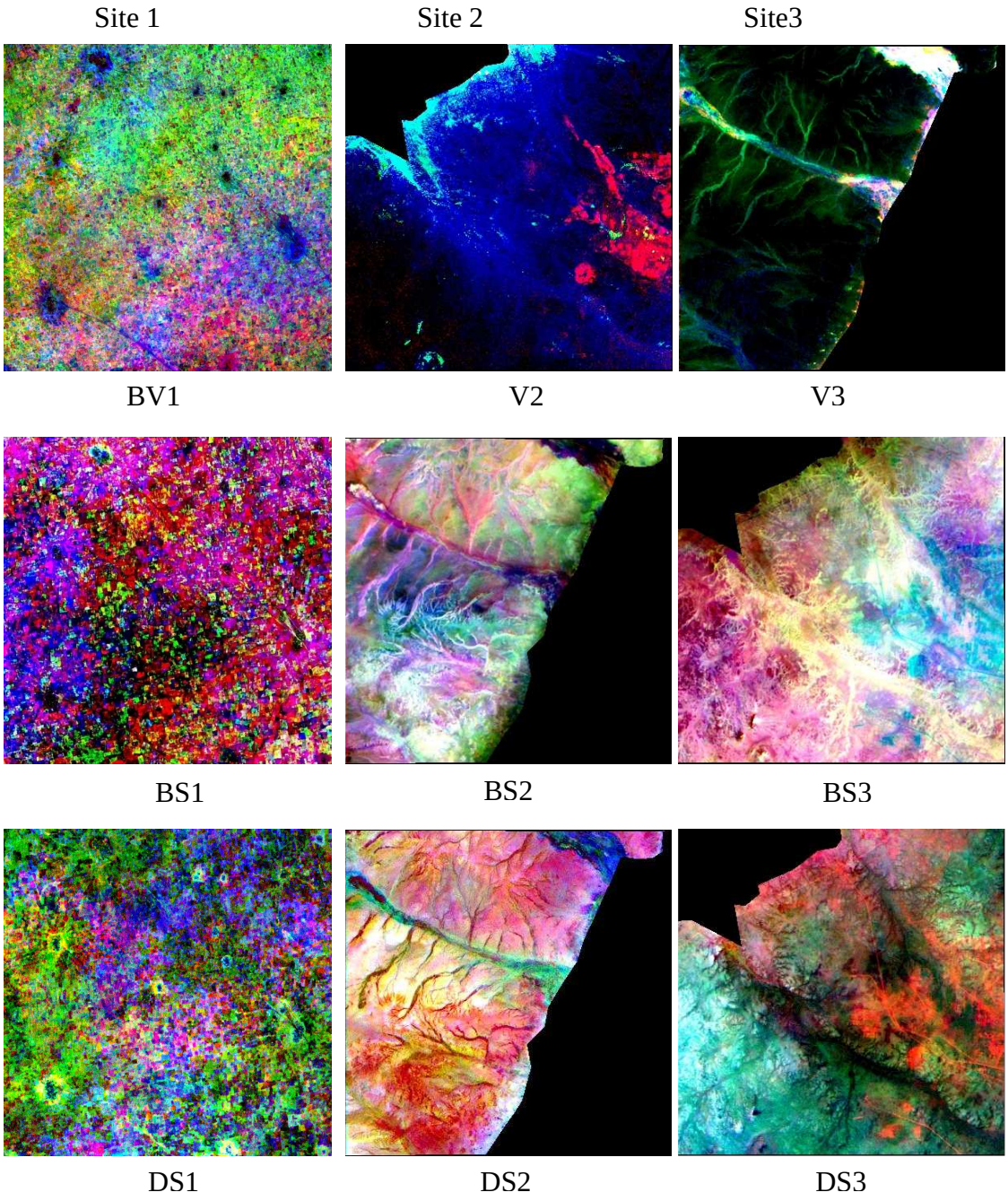

Figure 4.7- Displaying endmember fractions images for each site in stander BGR composite as year 1987 in blue, year1999 in green and year 2008 in red.

Vegetation fraction in general was higher in 1987 and 1999, mainly located around the villages in site 1 and along the valleys in site 2 and 3, indicating lost of vegetation in 2008. Figure 4.7 shows an increase in vegetation fraction due to the high rainfall in 1999 in the north-east part of site 1 and along the valleys in site 2 (saturated green color). High saturated blue appeared along the valley in site 3 indicating higher vegetation fraction in 1987. In 2008 vegetation fraction increased in a small scattered areas in site 1 and in a large eastern part in site 3 (red color), while stable condition were observed in downstream valley of site 2 (white color).

A drastic change of BS1 fraction can be observed in 2008 (Figure 4.7). It was spatially distributed around the villages and across the site from the northern to the eastern part. In site 2, DS2 fraction was high along the two main valleys in 1987 and 1999 (saturated blue and green color) but in 2008 increased in areas with sparse vegetation, mostly in the southern part. In the same part there were patches showing stable conditions (white color) for BS2. In site 3, BS3 fraction was higher in 1987 in the north eastern bank of the valley (saturated blue color) and in 2008 in the south western bank (red color), while it was steady along the valley (white color).

The fraction images of 1987 and 2008 were used in the application of CVA to identify the desertified and re-growth areas. BS1, BS2+DS2 and BS3 fractions were used in CVA equation to consider soil vulnerable to erosion while BV1, V2 and V3 fractions were used for vegetation.

According to CVA (Figures 4.8, 4.9 and 4.10), the magnitude of desertification in site 1 ranges from low to extreme, with a prevalence of severe degradation conditions (high or extreme) in the eastern part. Extreme status of desertification was observed in site 2 along the valleys and high to low in site 3. The percentages of the desertified areas are 48%, 25% and 76% out of the total area of site 1, 2 and 3 respectively. Change detection analysis shows the existence of low-medium re-growth conditions in site 1 (Figure 4.8), mostly spread in the south-western part, and in site 3 (Figure 4.10).

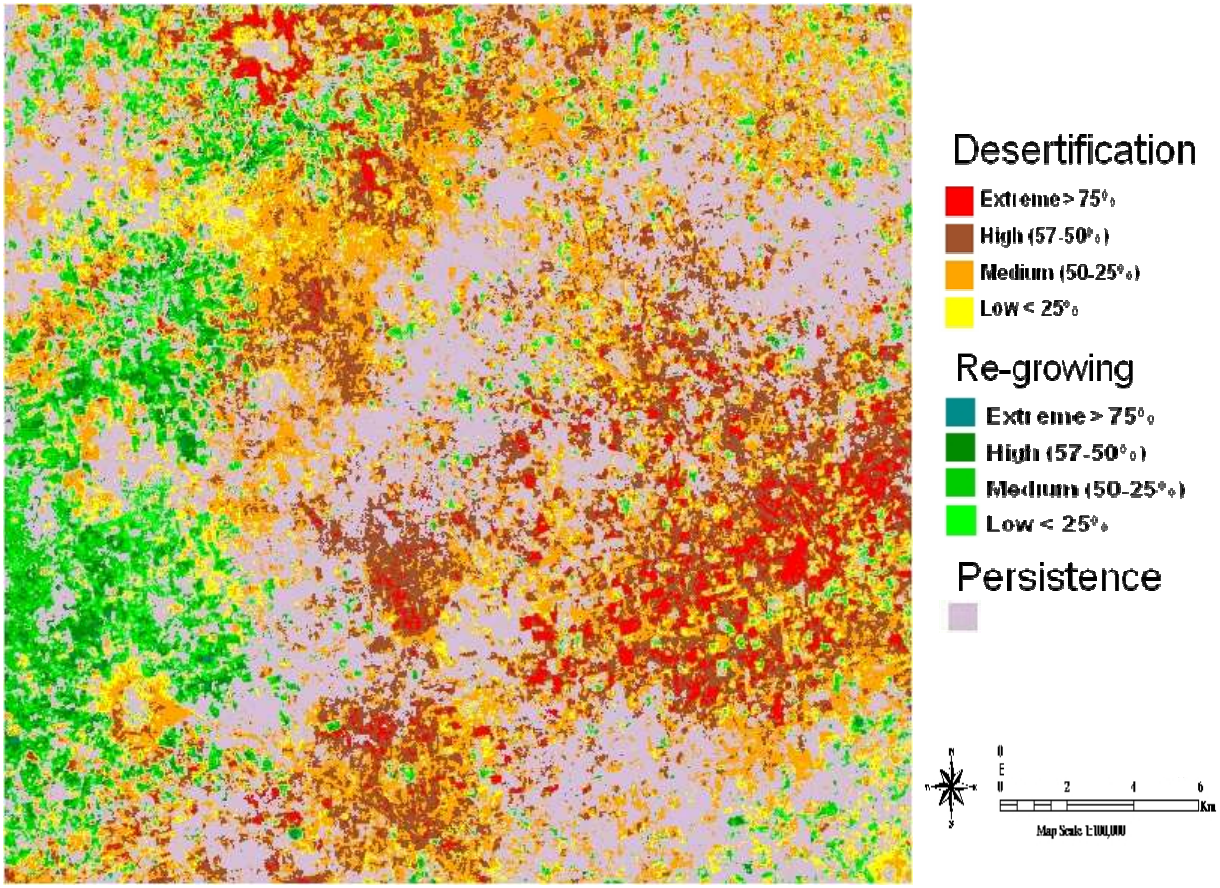

Figure 4.8 - Desertification and re-growth areas in site 1 calculated by applying change vector analysis.

Desertification prevailed over re-growth in site 1 affecting an area of 153,867 km^2, with a prevalence of medium (70,944 km^2) and high (48,578 km^2) classes of magnitude. Re-growth was estimated on an area of 35,313 km^2, mainly classified as medium (17,005 km^2) and low (13,708 km^2). In site 2 desertification was "extreme" over an area of 24,482 km^2 while low re-growth conditions characterized a restricted area of 1,193 km^2. The rest of the area, corresponding to desert core , was classified as persistence condition (71,298 km^2) (Figure 4.9). The highest percentage of desertified area (from low to high) was estimated in site 3, over an area of 98,275 km^2 corresponding to the 76% of the total surface.

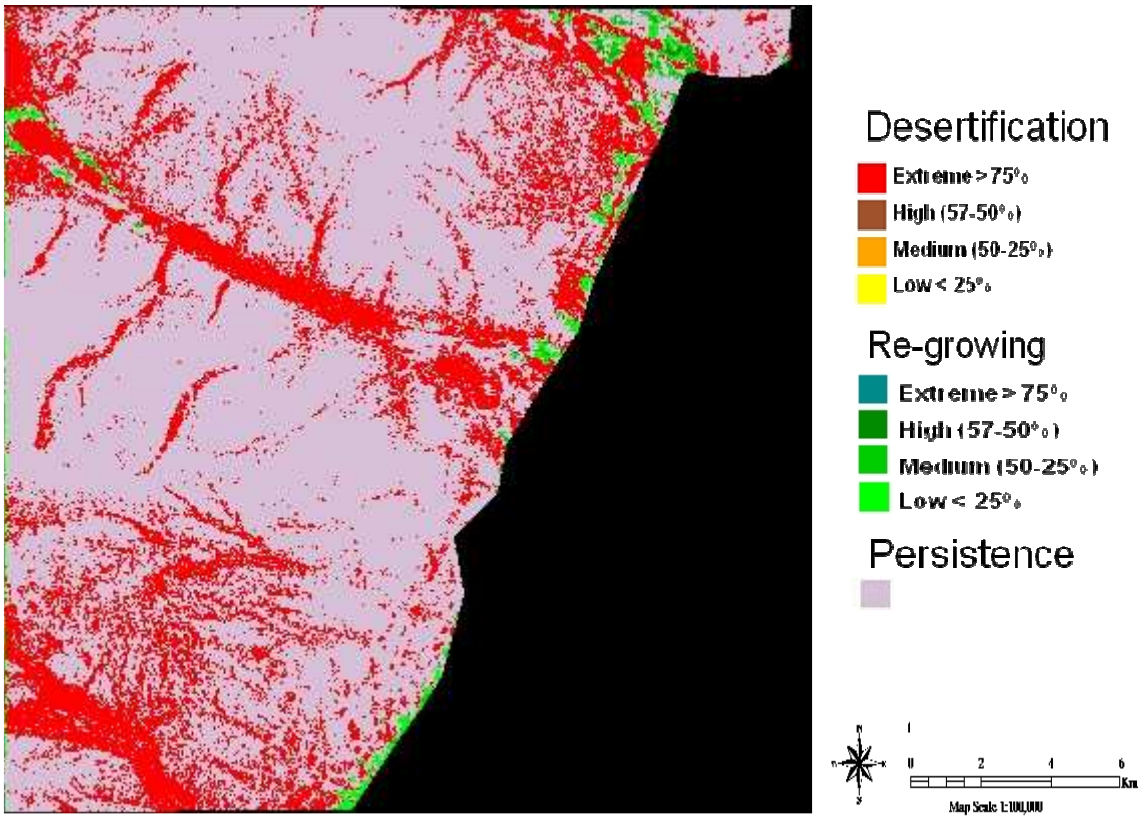

Figure 4.9- Desertification and re-growth areas in site 2 calculated by applying change vector analysis.

Different factors drove the desertification in the three areas. In site1, human activities strongly affected degradation phenomenon. First of all the expansion of villages triggered the change in land use and mismanagement of the natural resource, mainly caused by deforestation to supply wood for domestic uses i.e. building, cooking, etc., and overgrazing (Sherbinin, 2002). The degradation moreover promoted sand encroachment and dune migration, which are considered as one of the main processes of land degradation in arid regions (Balba, 1995). The conversion of rangeland into cultivated croplands is another phenomenon which affected the desertification in the site 1, especially in the southern part. The change in land use to cultivation led to a decrease in BV, especially in the central part and a contemporary massive increase in BS fraction. The conversion of dry and fragile rangelands into traditional and mechanized cropland has already been indicated by many Authors (e.g. Herrmann et al., 2005; Olsson et al., 2005) as one of the main processes affecting desertification in Sudan. Over-exploitation of semi-desert environments through deforestation, overgrazing and cultivation

results in habitat conversion to desert, even though rainfall may still be sufficient to support semi-desert vegetation (Nicholson, 2005). Desertification was partially compensated by the re-growth conditions observed in the SW part, which were mainly due to Government reforestation projects in last decade and sustained by higher rainfall in the last years in the study area. The Rainfall Anomaly Index (RAI) (Tilahun, 2006) time series (Figure 4.11) confirmed the existence of favourable conditions for vegetation growth from the 1990s to 2008, with higher frequency of positive anomalies than in the 1970s and 1980s. This result is in accordance with the recent satellite and model based studies of the Sahel (e.g. Eklundh and Olsson, 2003; Anyamba and Tucker, 2005), which demonstrated that vegetation has recovered from the peak drought conditions suffered in the region in the 1980s.

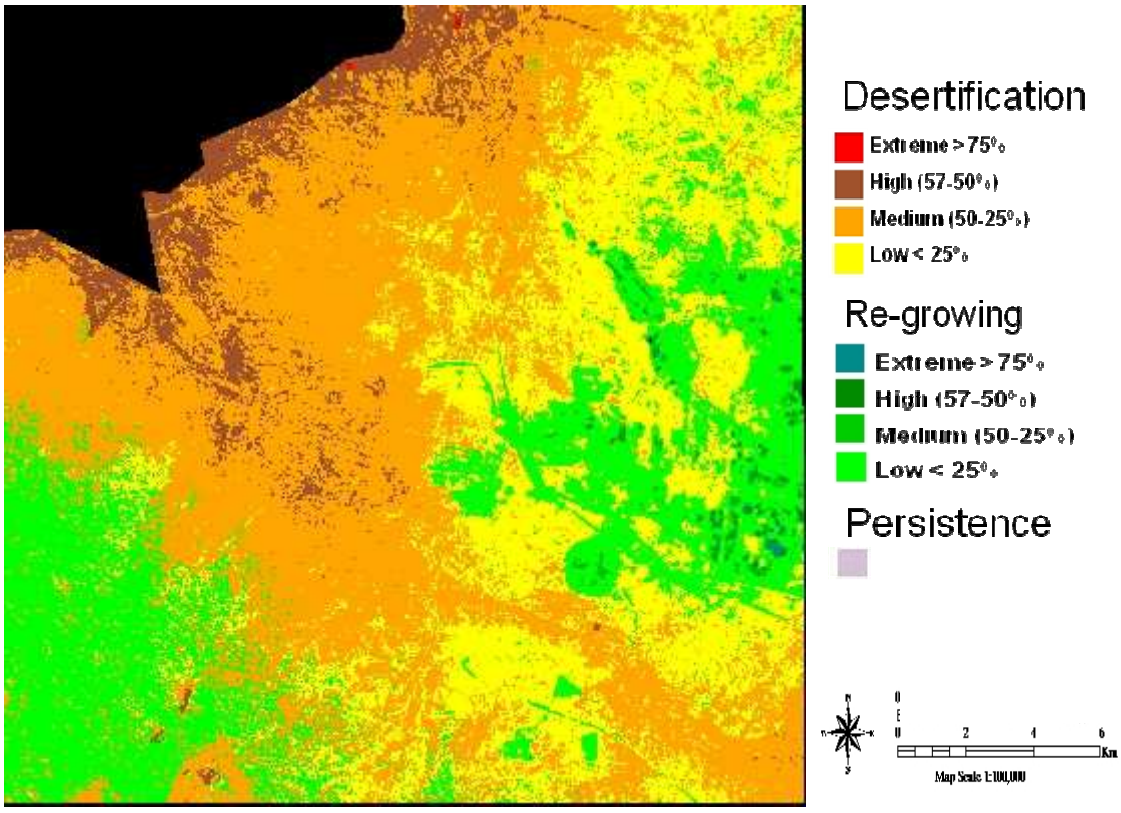

Figure 4.8 - Desertification and re-growth areas in site 3 calculated by applying change vector analysis.

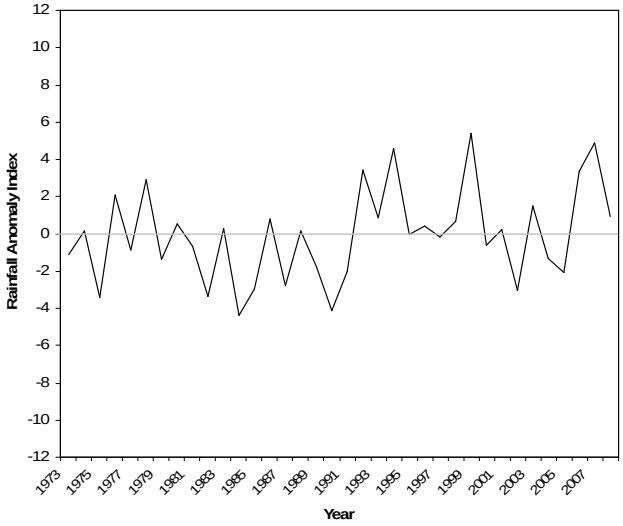

Site 1

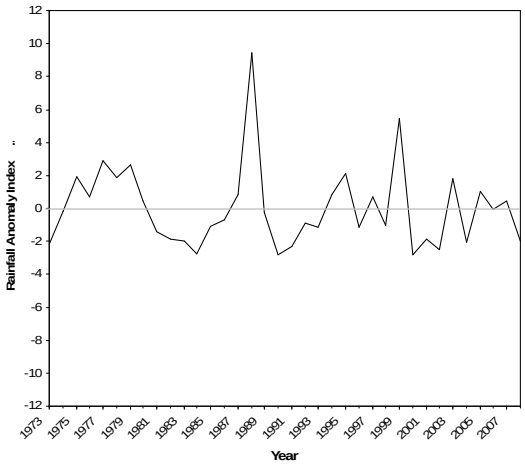

Site 2

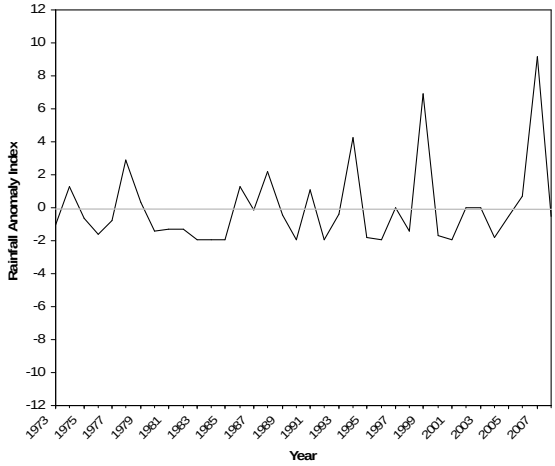

Site3

Figure 4.11- Rainfall Anomaly Index (RAI) from 1973 to 2008 for each site individually.

In different way climatic constrains drove desertification in sites 2 and 3. Drought, degradation and soil erosion were the causes and effects of desertification (Guoping et al., 2001). In particular, extreme desertification was observed along the valley in site2, where the progressive lost of vegetation could have enhanced soil degradation. In fact, vegetation along the valleys in the desert areas plays a very important role in reducing water erosion during the rainy season (Fenli et al., 2002) and wind erosion during the dry season (Bach, 1998). RAI time series for desert and semi-desert regions (Figure 4.11) confirmed the existence of drought period during the last 36 years. Indeed even if RAI in the last two decades registered higher anomalies than 1970s and 1980s, there was not a prevalence of positive anomalies such as those ones observed

for site 1. This condition explained the existence of the extreme condition of desertification in site 2 and the large diffusion of desertified area in site 3.

Moreover, in these sites re-growth conditions were observed only where forestry or agricultural projects were established. For instance in site 2 it was due to planting of *Prosopis chilensis* (Molina) Stuntz. and *Prosopis juliflora* (Sw.)DC. which were exotic and invasive (Salih and Mohamed, 2008). In site 3 the eastern re-growth area corresponded to few agricultural projects established in 2007, but that are considered to be unsustainable and at high risk (Okin and Roberts, 2004) since they are surrounded by desertified area.

4.4 Conclusions

A converging outlook about the causes and effects of drought, land degradation and desertification is still lacking. As pointed out by Herrmann et al. (2005) there are two competing schools representing diametrically opposed positions in this debate: one supports the hypothesis that human activities are responsible for a irreversible desertification in Sahel by "overuse of resources" and "human mismanagement" (e.g. Mainguet, 1991), the other interpreters the desertification as phenomenon driven by drought, and hence temporary, with humans playing a minor role (e.g. Olsson et al., 2005).

According to the results of this study it is not possible to support one or the other school. This study highlighted the complexity of desertification phenomenon: ecological zone patterns and natural resources strongly interact with human activities in semi-arid areas. The pressure on land, wherever wood and rainfall are available for energy and cultivation, was clearly observed in the semi-arid area. Human activities and mismanagement of the natural resource with expansion of the villages in Savanna region highly accelerated desertification processes in savanna site, but in semi-desert and desert sites, climate constraints were the main cause of degradation.

Site-specific strategies which take into account the interactions of the driving factors at local scale are thus necessary to combat desertification, avoiding any implementation of untargeted measures. In particular, an attention is needed to conserve valleys ecosystem in semi-desert and desert region in order to play its role in reducing wind and water erosion.

PART FIVE:
CONCLUSIONS AND RECOMMENDATIONS

5.1 Conclusions

Desertified area and desertification processes in North Kordofan, River Nile and Northern states were detected and the factors affecting this change was analysed using tempo-spatial analysis of the remote sensing data. The three selected sites were characterized by heterogeneous land use/land cover as in semi-arid areas. The amount of vegetation cover, types of dry ecosystem vegetation and structure and phenology of vegetation regarding to the harsh environment are found to be differ from one ecological zone to another and affect the contribution of vegetation reflectance in the total pixel reflectance relative to the other materials. Mineral and organic matter, soil structure and moisture content of the soil surface are the main factors affecting the reflectance of soil in the optical remote sensing.

The application of spectral mixture analysis (SMA) to Landsat data appeared to be a consistent, accurate and low-cost technique to obtain information on vegetation cover, soil surface type, and identify risk areas. In this study, Landsat ETM+7 OFF-SLC images were used after correction in SMA application and provided acceptable landcove/landuse (LCLU) fraction images. SMA proved to be a powerful technique in characterization and mapping of desertification processes in the study sites by providing direct measurements to different land cover at subpixel level. Endmembers spectra were successfully derived from Landsat images using the principle component (PC) and the method proved to be valuable. Although the results shows an overestimation errors, they were acceptable to evaluate the LULC change regarding the comparative approach of the present study. Applying endmember fractions of 1987 and 2008 to change vector analysis (CVA) showed desertification significantly prevailed over vegetation re-growth in the three sites.

Site-specific interactions between natural processes, climate variation and human activity play a pivotal role on desertification in the study sites. Even if phenomena at large scale (e.g. positive rainfall trend) in savannah site in the last years have allowed a gradual recovery from the peak drought conditions suffered in the Sahel during the 1980s, there are still forcing variables that act at local scale to cause land degradation. Drought condition have accelerated the desertification processes in semi-desert and desert sites since there was no positive continuous signal of rainfall trend in these sites during last 36 years. One of the most important factors affecting such degradation were human activities, which exploit the natural resources beyond their ecological resilience threshold until desertification is irreversible. Hunger and local energy needs seem to be the driver of land use and management. Site-specific strategies

that take into account the interactions of the driving factors at local scale are thus necessary to combat desertification, avoiding the implementation of untargeted measures. The following conclusions could be addressed according to the study:

- The spectral reflectance of vegetation in arid and semiarid areas changes with the vegetation structure and surrounding environment.
- Deriving Endmembers spectra from Landsat images, using the principle component (PC), is successful and valuable method.
- Applying Landsat ETM+7 OFF-SLC after correction in SMA proved to be valuable and accurate for monitoring desertification.
- SMA is a powerful technique in characterization and mapping of desertification processes in the study areas by providing direct measurements to different land cover at subpixel level.
- SMA distinguishes the effect of climate variation as well as the role human activities in accelerating desertification.
- Visual interpretation using the color composite of SMA fraction images is a practical and simple way to explain the changes in vegetation and soil fractions.
- CVA allows for further detection and quantifying of desertification processes in a degree of severity.
- Desertification status is extreme to moderate in savanna site, extreme in semi-desert site and high to low in the desert site.
- Human activity and mismanagement of natural resources are the main factors affecting desertification in savanna region.
- High increase of very fine soil in semi desert area will cause problem of dust storms in the country.
- The agricultural projects in desert region are within vulnerable area to desertification, so, they are unsustainable.

5.2 Limitations of the study

- Unavailability of spectrometer device for measuring spectral signature of land cover materials in the fields.
- Limitation Landsat bands caused limitation of applying endmembers spectra.
- Limitation of the field survey plots caused limitation in the accuracy.
- Single station of the climatic data for each site causes lag of spatial climatic data.
- Unavailability of high resolution imagery images to calibrate the endmembers spectra.

5.3 Recommendations

Management of natural resources in fragile ecosystems in the addressed study sites is highly recommended in order to control the desertification problem and to combat it. Using remote sensing for monitoring land degradation is the key tool to establish combating projects. The following recommendations are pointed out:

- Establishing remote sensing application units in the academic and research institutes and in the governmental agencies which responsible of desertification problem in Sudan to provide valuable information on land use/land cover of the regions subjected to desertification for the planner and decision maker.
- Since the desertification problem has complex factors, establishing network between different institutes care of these factors is seriously needed.
- Raising of building capacity of researchers in application of remote sensing environment will improve the use of remote sensing in the governmental agencies.
- In order to identify the soundest strategies, high-resolution tools must be applied.
- Revising the land use policies and strategies of settlements and sustainable development.
- At local scale, encouraging the national organizations along with the local population to work on re-planting the native species.
- Protecting the irrigated agricultural projects in desert areas by shelterbelts and windbreaks is seriously needed to sustain these activities.

- Improving and managing the grazing activities will help in avoiding reduction soil productivity.
- Improving the metrological station in space and accuracy to provide the monitoring system with the needed climatic data.
- Establishment an early warning systems is urgently needed.

5.4 Further studies

More effort should be made to improve the classification of vegetation type in order to distinguish perennial from annual species and thus be able to monitor long-term vegetation degradation. Hyperspectral imagery, spectrometry and long term field monitoring experiments for land cover strongly support this context and increase the accuracy of monitoring drylands.

References

Abdel Ati and Hassan A. (2002) Sustainable Development in Sudan. Ten Years After Rio Summit: A Civil Society Perspective. Solo Publishers, Khartoum, Sudan.

Adams J.B., Sabol D.E., Kapos, V., Almeida Filho R., Roberts D.A., Smith M.O. and Gillespie A.R. (1995) Classification of multispectral images based on fractions of endmembers: Applications to land-cover change in the Brazilian Amazon. Remote Sensing of Environment 52:137-154.

Adams J.B., Smith M.O. and Johnson P.E. (1986) Spectral mixture modeling: a new analysis of rock and soil types at the Viking Lander I Site. Journal of Geophysics Researches 91:8098-8112.

Ali M.M. and Bayoumi A.A.M.S. (2004) Assessment and mapping of desertification in western Sudan using remote sensing techniques and GIS, in: International Conf. on Water Resources and Arid Environment. PSIPW, Riyadh.

Anyamba A., and Tucker C.J. (2005) Analysis of Sahelian vegetation dynamic using NOAA-AVHRR NDVI data from 1981-2003. Journal of Arid Environments 63:596-614.

Asner G.P. (1998) Biophysical and biochemical sources of variability in canopy reflectance. Remote Sensing of Environment 64:234-253.

Asner G.P. (2004) Biophysical remote sensing signatures of arid and semiarid ecosystem, in: Ustin, S.L. (Ed.), Remote Sensing for Natural Resources Management and Environmental Monitoring. Third ed., Hoboken, New Jersey pp. 53-109.

Atta El Moula M.E. (1985) On the Problem of Resource Management in the Sudan. Environmental Monograph Series No. 4. Institute of Environmental Studies, University of Khartoum, Sudan.

Ayoub A. T. (2004) The Need for Systematic Monitoring and Assessment of Land Degradation/Desertification in the Sudan, United Nations Office for Outer Space Affairs, Vienna, Austria.

Ayoub Ali T. (1998) Extent, severity and causative factors of land degradation in the Sudan, Journal of Arid Environment 138:397-409.

Bach A. J. (1998) Assessing conditions leading to sever wing erosion in Antelope Valley, California, 1990-1991. Profecinal Geographer 50:87-97.

Balba, A.M. (1995) Management of Problem Soils in Arid Ecosystems. CRC Press, Boca Raton, Florida.

Bateson C.A. and Curtiss B. (1996) A method for manual endmember selection and spectral unmixing. Remote Sensing of Environment 55:229-243.

Bateson C.A., Asner G.P. and Wessman C.A. (2000) Endmember bundles: A new approach to incorporating endmember variability in spectral mixture analysis. IEEE Transactions on Geoscience and Remote Sensing 38:1083-1094.

Brandt J.S. and Townsend P.A. (2006). Land cover conversion, regeneration and degradation in the high elevation Bolivian Andes. Landscape Ecology 21:607-623.

Chavez P.S. (1988) An improved dark-object subtraction technique for atmospheric scattering correction of multispectral data. Remote Sensing of Environment 24:459– 479.

Collado D.A., Chuvieco E. and Camarasa A. (2002) Satellite remote sensing analysis to monitor desertification processes in the crop-rangeland boundary of Argentina. Journal of Arid Environments 52:121-133.

Crist E.P. and Cicone R.C. (1984) A physically-based transformation of Thematic Mapper data-the TM tasseled cap. IEEE Transactions on Geoscience and Remote Sensing 22:256-263.

Dafalla M.S. and Casplovics E. (2005) Applicability and limitations of land use / land cover classification using high resolution satellite imagery in arid and semi-arid areas of the Northern Kordofan State (Sudan) in: Roder A., Hill, J. (Eds.), Proceedings of the First International Conference on Remote Sensing and Geoinformation Processing in the Assessment and Monitoring of Land Degradation and Desertification. Trier, Germany pp. 549-555.

Dawelbait M. and Morari F. (2008) Limits and potentialities of studying dryland vegetation using the optical remote sensing. Italian Journal of Agronomy 3:97- 106.

De Asis A.M. and Omasa K. (2007) Estimation of vegetation parameter for modeling soil erosion using linear Spectral Mixture Analysis of Landsat ETM data. ISPRS Journal of Photogrammetry & Remote Sensing 62:309-324.

de Jong-Boon and Caroline (1990) Environmental Problems in the Sudan, Part I, The Hague.

DECARP (1976). Sudan desert encroachment control and rehabilitation program. Prepared jointly by the central administration for Natural Resources Ministry of Agricultural Council, National Council for Research in collaboration with UNEP and FAO, Khartoum, Sudan.

Diouf A. and Lambin E.F. (2001) Monitoring land cover changes in semi-arid regions: remote sensing data and field observations in the Ferlo, Senegal. Journal of Arid Environments 48:129–148.

Dorigo W.A., Zurita-Milla R., Wit A.J.W. de, Brazile J., Singh R., Schaepman M.E. 2007. A review on reflective remote sensing and data assimilation techniques for enhanced agroecosystem modelling. International Journal of Applied Earth Observation and Geoinformation, 9:165–193.

Drake N.A. and White K. (1991) Linear mixture modelling of Landsat Thematic Mapper data for mapping the distribution and abundance of gypsum in the Tunisian Southern Atlas, In Spatial data 2000, in: Dowman, I. (Ed.), Proceedings of a Joint Conference of the Photogrammetric Society, the Remote Sensing Society. The American Society for Photogrammetry and Remote Sensing, Christ Church, Oxford, pp. 168-177.

Dregne H.E. (1977) Desertification of arid lands. Economic Geography 53:329.

Ehleringer J.R. and Mooney H.A. (1978) Leaf hairs: effects on physiological activity and adaptive value to a desert shrub. Oecologia, 37:183-200.

Eklundh L. and Olsson, L. (2003). Vegetation index trends for the African Sahel 1982–1999. Geophysical Research Letters 30:1430.

Elmore A.J., Mustard J.F., Manning S.J. and Lobell D.B. (2000) Quantifying vegetation change in semiarid environments. Remote Sensing of Environment, 73:87-102.

FAO-UNEP (1984) Provisional Methodology for Assessment and Mapping of Desertification. FAO, Rome.

FAO-UNESCO (1997) Soil map of the world. Revised legend, World Soil Resources Report 60, FAO, Rome. Reprinted with updates as Technical Paper 20, ISRIC, Wageningen.

Fenli Z, Keli T, Cheng-e Z and Xiubin H. (2002) Vegetation Destruction and Restoration Effects on Soil Erosion Process on the Loess Plateau. 12th ISCO Conference, Beijing.

Franklin J., Duncan J. and Turner D.L. (1993) Reflectance of vegetation and soil in Chihuahuan desert plant communities from ground radiometry using SPOT wavebands. Remote Sensing of Environment, 46:291-304.

Graetz D. (1994) Grasslands. p. 125-147. In: W.B. Meyer and B.L. Turner II (eds), Changes in Land Use and Land Cover: A Global Perspective. Cambridge University Press, Great Britain.

Guoping Z., Zengxiang Z. and Liyuan L. (2001) Spatial gistribution of wing erosion and its driving factors in China. Journal of Geographical science. 11:127-139.

Haralick R.M and Fu K.S. (1983) Pattern recognition and classification. In: Cowell R.N., (ed.): Manual of Remote Sensing, 2:793-806. 2nd edition, American Society of Photogramm, Fails Church, Virginia.

Harrison M.N and Jackson J.K (1958). Ecological classification of vegetation cover of Sudan.

Hassan H. and Luscombe W. (1990) Disaster information and technology transfer in developing countries, in: Kreimer, A., Munasinghe, M. (Eds.), Proceedings of the Colloquium on the Environment and Natural Disaster Management. World Bank, Washington, pp. 141-144.

Hellden U. (2008) A coupled human-environment model for desertification simulation and impact studies. Global and Planetary Change 64, 158-168.

Herrmann S.M., Anyamba A. and Tucker C.J. (2005) Recent trends in vegetation dynamics in the African Sahel and their relationship to climate. Global Environment Change 15:394-404

Huete A. (2004) Remote sensing of soil and soil processes, in: Ustin, S.L. (Ed.), Remote Sensing for Natural Resources Management and Environmental Monitoring. Third ed., Hoboken, New Jersey pp. 3-52.

Huete A.R. (1988) A soil-adjusted vegetation index (SAVI). Remote Sensing of Environment, 25:295-309.

Huete A.R. and Jackson R.D. (1987) Suitability of spectral indices for evaluating vegetation characteristics on arid rangelands. Remote Sensing of Environment, 23:213-232.

Huete A.R., van Leeuwen W.J.D., Hua G., Qi J. and Chehbouni A. (1992) Normalization of multidirectional red and NIR reflectances with the SAVI. Remote Sensing of Environment 41:143-154.

Hurcom S.J. and Harrison A.R. (1998) The NDVI and spectral decomposition for semiarid vegetation abundance estimation. International Journal of Remote Sensing 19:3109-3125.

Jackson R.D., Slater P.N. and Pinter P.J. (1983) Discrimination of growth and water stress in wheat by various vegetation indices through clear and turbid atmospheres. Remote Sensing of Environment 13:187-208.

Jensen R.J. (2005) Remote Sensing of Environment. 3rd edition, Pearson education, Delhi.

Johnson, P.E., Smith, M.O. and Adams, J.B. (1985) Quantitative analysis of planetary reflectance spectra with principal components analysis. Journal of Geophysical Research 90:C805-C810.

Khiry M.A. (2007) Spectral Mixture Analysis for Monitoring and Mapping Desertification Processes in Semi-arid Areas, first ed. Rhombos-Verlag, Berlin.

Kuzera K., Rogan, J. and Eastman J.R., (2005) Monitoring vegetation regeneration and deforestation using change vector analysis: MT. ST. Helens study area, in: ASPR 2005 Annual Conference. Baltimore, Maryland.

Lal R. (1994) Methods and Guidelines for Assessing Sustainable Use of Soil and Water Resources in the Tropics. SMSS Technical Monograph No. 21. 78 pp. Washington, D.C.: NRCS

Le Houerou H.N. (2006) Desertization, in: Lal, R. (Ed.), Soil Science. CRC Press, Boca Raton, Florida pp. 468-474.

Lillesand T.M., Kiefer R.W. and Chipman J.W. (2004) Remote Sensing and Image Interpretation, fifth ed. Las Vegas. New York.

Lonergan S. (2005). The role of UNEP in desertification research and mitigation. Journal of Arid Environments 63:533–534.

Lu D., and Weng Q. (2004) Spectral Mixture Analysis of the urban landscape in Indianapolis with Landsat ETM+ imagery. Photogrammetric Engineering & Remote Sensing 70:1053-1062.

Mabbutt J.A. (1986) Desertification indicators. Climatic Change 9:113-122.

Mainguet M. (1991) Desertification: Natural Background and Human Mismanagement. Springer, Berlin.

Malila W.A. (1980) Change vector analysis: an approach for detecting forest changes with Landsat, in: Proceedings of the 6th Annual Symposium on Machine Processing of Remotely Sensed Data. Purdue University, West Lafayette, IN pp. 326-335.

Markham B.L. and Barker, J.L. (1986) Landsat MSS and TM post-calibration dynamic ranges, exoatmospheric reflectances and at-satellite temperatures. EOSAT Landsat Technical Notes No.1.

Moran M.S., Bryant R., Thome K., Ni W., Nouvellon Y., Gonzalez-Dugo M.P. and Qi, J. (2001) A refined empirical line approach for reflectance factor retrieval from Landsat-5 TM and Landsat-7 ETM+. Remote Sensing of Environment 78:71–82.

Mustafa M.A. (2007) Desertification Processes, first ed. Khartoum University Press, Khartoum.

Nicholson S. (2005) On the question of the ‘‘recovery’’ of the rains in the West African Sahel. Journal of Arid Environments 63:615–641.

Okin G.S., Okin W.J., Murray B. and Roberts D.A. (2001) Practical limits on hyperspectral vegetation discrimination in arid and semiarid environments. Remote Sensing of Environment, 77:212-225.

Okin G.S., Robert D.A. 2004. Remote sensing in arid regions: challenges and opportunities, in: Ustin, S.L. (Ed.), Remote Sensing for Natural Resources Management and Environmental Monitoring. Third ed., Hoboken, New Jersey pp. 111-145.

Oldeman L.R., Hakkeling R.T.A. and Sombroek W.G. (1991) Global Assessment of Human-induced Soil Degradation (GLASOD). World map of the status of human-induced soil degradation. Winand Staring Centre- ISSS-FAO-ITC (eds.) 41 pp.

Olsson L., Eklundh, L. and Ardoe J. (2005) A recent greening of the Sahel trends, patterns and potential causes. Journal of Arid Environments 63:556–566.

Phinn S., Franklin J., Hope A., Stow D. and Huenneke L. (1996) Biomass distribution mapping using airborne digital video imagery and spatial statistics in a semi-arid environment. Journal of Environmental Management 47:139-164.

Pickup G. (1995) A simple model for predicting herbage production from rainfall in rangelands and its calibration using remotely-sensed data. Journal of Arid Environments 30:227–245.

Qin W. and Gerstl S.A.W. (2000) 3-D scene modelling of semi-desert vegetation cover and its radiation regime. Remote Sensing of Environment 74:145-162.

Ray T.W. and Murray B.C. (1996) Nonlinear spectral mixing in desert vegetation. Remote Sensing of Environment 55:59-64.

Reich P.F., Numbem S.T., Almaraz R.A. and Eswaran H. (2001) Land resource stresses and desertification in Africa. In: Bridges, E.M., I.D. Hannam, L.R. Oldeman, F.W.T. Pening de Vries S.J., Scherr and S. Sompatpanit (eds.). Responses to Land Degradation. Proc. 2nd. International Conference on Land Degradation and Desertification, Khon Kaen, Thailand. Oxford Press, New Delhi, India.

Ringrose S., Matheson W., Mogotsi B. and Tempest F. (1989) The darkening effect in drought affected savanna woodland environments relative to soil reflectance in Landsat and SPOT wavebands. Remote Sensing of Environment 30:1–19.

Roberts D.A., Gardner M., Church R., Ustin S., Scheer G. and Green R.O. (1998) Mapping chaparral in the Santa Monica Mountains using multiple endmember spectral mixture models. Remote Sensing of Environment 65:267-279.

Roberts D.A., Smith M.O. and Adams J.B. (1993) Green vegetation, non-photosynthetic vegetation, and soils in AVIRIS data. Remote Sensing of Environment 44:255- 269.

Rozanov and Boris G. (1990). Global assessment of desertification: Status and methodologies. Proceedings of an Ad-Hoc Consultative Meeting on the Assessment of Desertification, UNEP, Nairobi.

Rubio J.L. and Bochet E. (1998) Desertification indicators as diagnosis criteria for desertification risk assessment in Europe. Journal of Arid Environments 39:113-120.

Scaramuzza P., Micijevic E. and Chander G. (2004) SLC gap-filled products phase one methodology. Landsat Technical Notes.

Sherbinin D.S. (2002) A CIESIN Thematic guide to Land-use and Land-cover Change (LUCC). Columbia University, Palisades, NY.

Singh G. (2009) Salinity-related desertification and management strategies: Indian experience. Land Degradation & Development 20:367-385.

Smith M.O., Johnson P.E. and Adams J.B. (1985) Quantitative determination of mineral types and abundances from reflectance spectra using principal components analysis, in: Ryder G., Schubert G. (ed.): Proceedings 15th Lunar and Planetary Science Conference, 14-16 March 1984. American Geophysical Union, Houston, Texas C797-C804.

Smith M.O., Ustin S.L., Adams J.B. and Gillespie A.R. (1990a). Vegetation in deserts: I. A regional measure of abundance from multispectral images. Remote Sensing of Environment 31:1-26.

Smith M.O., Ustin S.L., Adams J.B. and Gillespie A.R. 1(990b) Vegetation in deserts: II. Environmental influences on regional abundance. Remote Sensing of Environment 31:27-52.

Theseira M.A., Thomas G., Taylor J.C. Gemmell F. and Varjo J. (2003) Sensitivity of mixture modelling to endmember selection. International Journal of Remote Sensing 24:1559-1575.

Tilahun K. (2006) Analysis of rainfall climate and evapo-transpiration in arid and semi-arid regions of Ethiopia using data over the last half a century. Journal of Arid Environment 64:474-487.

Tompkins S., Mustard J.F., Pieters C.M. and Forsyth D.W. (1997) Optimization of endmembers for spectral mixture analysis. Remote Sensing of Environment 59:472-489.

Trodd N.M. and Dougill A.J. (1998) Monitoring vegetation dynamics in semi-arid African rangelands. Applied Geography 18:4:315–330.

Tucker C.J. (1979) Red and photographic infrared linear combinations for monitoring vegetation. Remote Sensing of Environment 8:127-150.

Tueller P.T. and Oleson S.G. (1989) Diurnal radiance and shadow fluctuations in a cold desert shrub plant community. Remote Sensing Environment 29:1-13.

UNCCD (1994) Status of Ratification and Entry into Force. United Nations Convention to Combat Desertification, Paris.

UNEP (2007) Sudan Post-Conflict Environmental Assessment. United Nations Environment Programme, Geneva.

Ustin S.L., Adams J.B., Elvidge C.D., Rejmanek M., Rock B.N., Smith M.O., Thomas R.W. and Woodward R.A. (1986) Thematic mapper studies of semiarid shrub communities. BioScience, 36:446-452.

Ustin S.L., Zarco-Tejada P.J., Jacquemoud S. and Asner G.P. (2004) Remote sensing of environment: state of science and new directions. In: Ustin S.L. (ed.): Remote Sensing for Natural Resources Management and Environmental Monitoring, 679-728. 3rd edition, WILEY, New Jersey.

Van Leeuwen W.J.D. and Huete A.R. (1996) Effects of standing litter on the biophysical interpretation of plant canopies with spectral indices. Remote Sensing of Environment, 55:123-134.

Villeneuve P.V., Gerstl S.A. and Asner G.P. (1998) Estimating nonlinear mixing effects for arid vegetation scenes with MISR channels and observation directions. In: CH 36042 (ed.): Proceedings of the International Geoscience and Remote Sensing Symposium, 3-8 August 1997, Singapore 3:31-35.

Virmani S.M., Katyal J.C., Eswaran H. and Abrol I. (1994) Stressed Agroecosystems and Sustainable Agriculture. New Delhi: Oxford & IBH.

Wessman C.A., Bateson C.A. and Benning T.L. (1997) Detecting fire and grazing patterns in tallgrass prairie using spectral mixture analysis. Ecological Applications 7:493-512.

White M.A., Asner G.P., Nemani R.R., Privette J.L. and Running S.W. (2000) Monitoring fractional cover and leaf area index in arid ecosystems: digital camera, radiation transmittance, and laser altimetry results. Remote Sensing of Environment 74:45-57.

Wiggs G.F.S., Thomas D.S.G. and Bullard J.E. (1995) Dune mobility and vegetation cover in the southwest Kalahari Deser. Earth Surface Processes and Landforms 20:515-529.

Wu C. (2004) Normalization spectral mixture analysis for monitoring urban composition using ETM+ imagery. Remote Sensing of Environment 93:480-492.

Acknowledgments

There are many people who contribute directly or indirectly by supporting me to accomplish this study. I admire Department of Environmental Agronomy and crop Production (DAAPV) - University of Padova for the hosting of this study as well as Government of the Sudan for giving me permission to study in Italy.

I am extremely grateful to my supervisor, Prof. Francesco Morari who has patiently guided the complicated case of remote sensing and arid areas and building up honestly my experience in this field. I express my gratitude also to the Head of Doctoral School, Prof Andrea Battisiti, for his real support and valuable suggestion during my stay in Italy.

The scholarship for my study came from the Italian Ministry of Foreign Affairs (Direzione Generale Cooperazione Allo Sviluppo), to which I owe a great deal of thanks, without their funding, this study would not have been possible. My sincere gratitude to my PhD colleagues in the Doctoral school and DAAPV staff as well.

My gratefulness is due to my colleges in the Ministry of Environment and Physical Development and many spatial thanks to Dr Elfadel Ali Adam, the Undersecretary, and Mamoun Esa Abdelqader, the Head of the Environmental Affairs, who honestly helped me in finding such opportunity. Appreciations are due to Forest National Corporation FNC – Sudan and my special gratitude goes to Dr. Abdallah Gaafer, the Chief Technical Sector, without his invaluable helpful to in conducting the field this study would not have been possible. Thanks are extended to FNC in Umruwaba, Marawi and Aldamer for their help and kind hospitality.

I am very grateful to the Universitario Center Directors in Padova, Don Roberto Ravazzolo and Don Marco Barcaro, as well as all the members in the Residence for the accommodation and likable friendly atmosphere. They are excellent people and a wonderful team who put extraordinary effort to make these years in Padova a pleasant stay and experience for me. I am indebted to Prof Davide Pettenella and his family for their kind hospitality.

Finally, I would like to thank my friends and family for believing in me, their encouragement for studying, and their understanding for the time that I could not spend with them because of my research responsibilities. Without the support of all of them, I could not have completed my PhD. study. Thanks God who gave me the life and all these people and opportunities.